

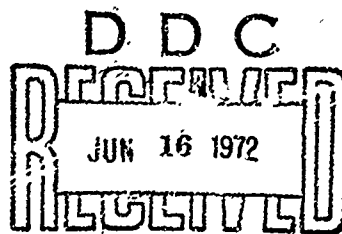
AD 43479

AN EXPERIMENTAL AND THEORETICAL
INVESTIGATION OF CONIC ENTRANCE
GRIFICE PERFORMANCE IN THE LOW
REYNOLDS NUMBER DOMAIN

A Research and Development Report
NAVSECPHILADIV PROJECT A-1000
SF 35 433 008, Task 03950
18 April 1972

**NAVAL SHIP ENGINEERING CENTER,
PHILADELPHIA DIVISION**

PHILADELPHIA, PA. 19112



Reprinted by
NATIONAL TECHNICAL
INFORMATION SERVICE
Springfield, Va 22151

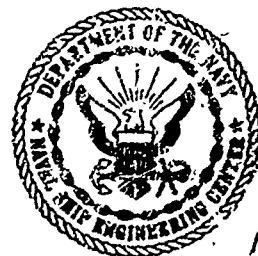
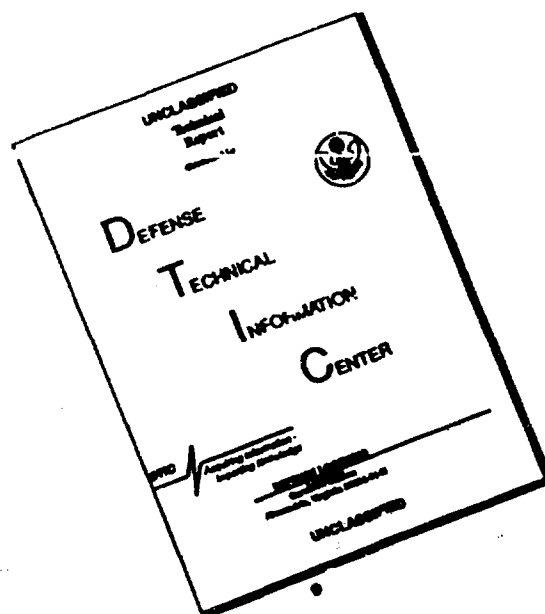


PLATE NO. 10917

Approved for public release; distribution unlimited

DISCLAIMER NOTICE



THIS DOCUMENT IS BEST
QUALITY AVAILABLE. THE COPY
FURNISHED TO DTIC CONTAINED
A SIGNIFICANT NUMBER OF
PAGES WHICH DO NOT
REPRODUCE LEGIBLY.

UNCLASSIFIED

Security Classification

DOCUMENT CONTROL DATA - R & D

(Security classification of title, body of abstract and indexing annotation must be entered when the overall report is classified)

ORIGINATING ACTIVITY (Corporate author)

Officer in Charge
 Naval Ship Engineering Center
 Philadelphia Division

2a. REPORT SECURITY CLASSIFICATION

UNCLASSIFIED

2b. GROUP

3. REPORT TITLE

An Experimental and Theoretical Investigation of Conic Entrance Orifice
 Performance in the Low Reynolds Number Domain

4. DESCRIPTIVE NOTES (Type of report and, inclusive dates)

A Research and Development Report

5. AUTHOR(S) (First name, middle initial, last name)

Ronald F. Bruner

6. REPORT DATE

18 April 1972

7a. TOTAL NO OF PAGES

36

7b. NO OF REFS

1

8a. CONTRACT OR GRANT NO.

8. PROJECT NO. NAVSECPHILADIV PROJECT A-1000

SF 35 433 008

4. Task 03950

9a. ORIGINATOR'S REPORT NUMBER(S)

NAVSECPHILADIV PROJECT A-1000

9b. OTHER REPORT NO(S) (Any other numbers that may be assigned this report)

10. DISTRIBUTION STATEMENT

Approved for public release; ~~distribution~~ unlimited

11. SUPPLEMENTARY NOTES

12. SPONSORING MILITARY ACTIVITY

Naval Ship Engineering Center
 Department of the Navy

13. ABSTRACT

A constant discharge coefficient (C_d), relating flow rate to the square root of the differential pressure across a primary element, is a desirable characteristic of any flow sensor to be used in shipboard automatic control systems. Although the simple, square edged orifice meets this criterion for turbulent flows, C_d does not remain constant for applications in the laminar and transitional regions of pipe Reynolds number (Re_D). In a quest for a device which exhibits both simplicity and a constant C_d at low Re_D , twelve conic entrance orifice plates were tested.

The range of orifice to pipe diameter ratios (β) was 0.1 to 0.5, and Re_D ranged from 40 to 50,000. C_d was constant within $\pm 1\%$ over the specified range of Re_D for $\beta = 0.1$. For $\beta \geq 0.2$, C_d was constant within $\pm 2\%$, indicating a worsening of performance with increasing β .

Graphs of C_d versus Re_D exhibited a "hump" which consistently occurred just below the critical Reynolds number for pipe flow (~ 2000). Theoretical considerations showed that this hump is attributable to fluid viscosity and that its height might be lessened by geometrical modifications. Accordingly, qualitative arguments are presented which contend that a protruding conic edge might improve performance at low Re_D .

The conic entrance orifice is to be preferred to the square edged orifice where low values of Re_D are encountered. The device is not unique, however, since quadrant edge orifices are also well suited for such measurements.

DD FORM 1473

(PAGE 1)

NOV 72 0101-007-0011

UNCLASSIFIED

Security Classification

A-31400

UNCLASSIFIED

Security Classification

KEY WORDS	LINK A		LINK B		LINK C	
	ROLE	WT	ROLE	WT	ROLE	WT
DESCRIPTORS						
CONTC ENTRANCE ORIFICE						
FLOW MEASUREMENT						
LOW REYNOLDS NUMBERS						
CONSTANT DISCHARGE COEFFICIENT						

DD FORM 1473 (BACK)
1 NOV 63
S/R DTIC-807-6821

UNCLASSIFIED
Security Classification

A-317

AN EXPERIMENTAL AND THEORETICAL
INVESTIGATION OF CONIC ENTRANCE
ORIFICE PERFORMANCE IN THE LOW
REYNOLDS NUMBER DOMAIN

A Research and Development Report
NAVSECPHILADIV Project A-1000
SF 35 433 008, Task 03950
18 April 1972

by

R. F. Bruner

APPROVAL INFORMATION

Submitted by:

J. S. Castorina
J. S. CASTORINA
Head, Fluid Dynamics & Metrology Section
Applied Physics Department

C. Gregory
C. GREGORY
Head, Scientific Branch
Applied Physics Department

J. W. Murdock
J. W. MURDOCK
Head, Applied Physics Department

Approved by:

J. C. Reaves
J. C. REAVES
Commander, USN
Director for
Machinery Engineering

Details of illustrations in
this document may be better
studied on microfiche

Approved for public release; distribution unlimited

TABLE OF CONTENTS

	<u>Page</u>
ABSTRACT	i
SUMMARY PAGE	ii
ADMINISTRATIVE INFORMATION	iv
NOMENCLATURE	v
REPORT OF INVESTIGATION	1
Introduction	1
Some Theoretical Background	3
Experimental Program	4
Test Results	12
Analysis	28
Conclusions	33
Recommendations	34
BIBLIOGRAPHY	35
APPENDIX A	
Specified and Measured Values of Conic Entrance Orifice Plate Dimensions	A1
APPENDIX B	
Simplified Solution for Potential Flow Through An Orifice	B1
APPENDIX C	
Correction to Discharge Coefficient Due to Laminar Upstream Velocity Profile	C1
LIST OF TABLES	
Table I - Range of Pipe Reynolds Numbers as a Function of Diameter Ratio R	2
Table II - Percentage Variation in C_d Over Prescribed Range of Re_D	12

TABLE OF CONTENTS (Cont'd)

	<u>Page</u>
LIST OF FIGURES	
Figure 1 - Section of Conic Entrance Orifice	5
Figure 2 - Upstream Face of Conic Entrance Orifice	6
Figure 3 - Cross Section Diagram of Taylor Flange Assembly	7
Figure 4 - Oil/Water Interface Reservoirs	9
Figure 5 - Test Set-Up	11
Figure 6 - Data from Daniel Plate with Nominal R Value of 0.1	13
Figure 7 - Data from Taylor Plate #2 with Nominal ρ Value of 0.1	14
Figure 8 - Data from Taylor Plate #1 with Nominal ρ Value of 0.1	15
Figure 9 - Data from Daniel Plate with Nominal R Value of 0.2	16
Figure 10 - Data from Taylor Plate #3 with Nominal ρ Value of 0.2	17
Figure 11 - Data from Taylor Plate #7 with Nominal ρ Value of 0.2	18
Figure 12 - Data from Daniel Plate with Nominal ρ Value of 0.3	19
Figure 13 - Data from Taylor Plate #4 with Nominal ρ Value of 0.3	20
Figure 14 - Data from Daniel Plate with Nominal ρ Value of 0.4	21
Figure 15 - Data from Taylor Plate #5 with Nominal ρ Value of 0.4	22
Figure 16 - Data from Daniel Plate with Nominal ρ Value of 0.5	23
Figure 17 - Data from Taylor Plate #6 with Nominal ρ Value of 0.5	24

TABLE OF CONTENTS (Cont'd)

	<u>Page</u>
Figure 18 - Discharge Coefficients Plotted Versus Throat Reynolds Number	27
Figure 19 - Section of Protruding Conic Edge Orifice	32
DISTRIBUTION	36

ABSTRACT

A constant discharge coefficient (C_d), relating flow rate to the square root of the differential pressure across a primary element, is a desirable characteristic of any flow sensor to be used in shipboard automatic control systems. Although the simple, square edged orifice meets this criterion for turbulent flows, C_d does not remain constant for applications in the laminar and transitional regions of pipe Reynolds number (Re_D). In a quest for a device which exhibits both simplicity and a constant C_d at low Re_D , twelve conic entrance orifice plates were tested.

The range of orifice to pipe diameter ratios (β) was 0.1 to 0.5, and Re_D ranged from 40 to 50,000. C_d was constant within $\pm 1\%$ over the specified range of Re_D for $\beta = 0.1$. For $\beta \geq 0.2$, C_d was constant within $\pm 2\%$, indicating a worsening of performance with increasing β .

Graphs of C_d versus Re_D exhibited a "hump" which consistently occurred just below the critical Reynolds number for pipe flow (~ 2000). Theoretical considerations showed that this hump is attributable to fluid viscosity and that its height might be lessened by geometrical modifications. Accordingly, qualitative arguments are presented which contend that a protruding conic edge might improve performance at low Re_D .

The conic entrance orifice is to be preferred to the square edged orifice where low values of Re_D are encountered. The device is not unique, however, since quadrant edge orifices are also well suited for such measurements.

SUMMARY PAGE

The Problem

A constant discharge coefficient (C_d), relating flow rate to the square root of the differential pressure across a primary element, is a desirable characteristic of any flow sensor to be used in shipboard automatic control systems. Although the simple, square edged orifice meets this criterion for turbulent flows, C_d does not remain constant for applications in the laminar and transitional regions of pipe Reynolds number (Re_D). A modified orifice for which C_d remains constant at low Re_D (i.e., into the laminar region) would thereby contribute to Naval flow measuring capabilities. Accordingly, it is the aim of this project to investigate the performance of the conic entrance orifice as a flow measuring element in the low Re_D domain covering laminar, transitional and turbulent pipe flows.

A secondary aim is to decipher which modifications to this type of orifice are likely to result in improved performance over the specified Reynolds number range.

Findings

While the conic entrance orifice is an improvement over the square edged orifice for flow measurement in the low Reynolds number domain, it is only for the smallest orifice-to-pipe diameter ratio tested, $R = 0.1$, that C_d may safely be assumed constant within $\pm 1\%$ maximum variation. For $R \geq 0.2$, the discharge coefficient may be considered constant within $\pm 2\%$. Further, a plot of discharge coefficient versus β with less than 1% standard deviation does not appear feasible for the specified range of Reynolds number.

Theoretical considerations suggest that modification of the upstream surface of the conic entrance orifice plate, producing a protruding conic edge, could result in improved performance at low Reynolds numbers.

Recommendations

The conic entrance orifice is preferable to a square edged orifice wherever pipe Reynolds numbers below 2000 are common. The device is not unique, however, since the quadrant edge orifice shows approximately the same percentage maximum variation in discharge coefficient over the specified range of Reynolds number.

Further investigations should involve testing of modified conic entrance orifice plates, such as the protruding conic edge orifice proposed in this report.

NAVSECPHILADIV PROJECT A-1000

ADMINISTRATIVE INFORMATION

This project was authorized by reference (a). Costs were charged to SF 35 433 008, Task 03950. This is a final report.

Reference

(a) NAVSECPHILADIV Semi-Annual Program Summary of 1 Oct 1969 (NOTAL)

NOMENCLATURE

A - area
 C_d - discharge coefficient
 D - pipe diameter
 d - orifice diameter
 m - mass flow rate
 P - pressure
 Re_D - pipe Reynolds number
 Re_d - throat Reynolds number
 v - fluid velocity

Greek

β - the ratio d/D
 ρ - fluid mass density

Subscripts

1 - denotes upstream station
 2 - denotes downstream station
 a - actual
 t - theoretical

REPORT OF INVESTIGATION

INTRODUCTION

The common square edged orifice, consisting of a concentric hole in a circular metal plate, is, geometrically, an exceedingly simple device for the measurement of fluid flow. If the Reynolds number (Re_D) of the flow is sufficiently large, then application of Bernoulli's equation leads to a theoretical expression for the mass flow rate which is equally simplistic, and is directly proportional to the actual mass flow rate. The "constant" of proportionality, C_d , is known as the discharge coefficient, and is actually a weak function of the Reynolds number, asymptotically approaching a constant value as $Re_D \rightarrow \infty$. If the upstream edge of an ordinary orifice is beveled, it is called a conic entrance orifice. For sufficiently large Re_D such an orifice lends itself to the same simplified flow measuring procedure described above for the squared edged orifice. However, in the low Reynolds number domain, when C_d can no longer safely be assumed independent of Re_D , the dependence of C_d on Re_D is different for the square edged and conic entrance orifices.

Since the magnitude of the deviation of C_d from its mean determines the lower limit of Re_D for which the Bernoulli equation approach will lead to accurate flow measurement, any modification to an ordinary orifice which results in a smaller variation in C_d at low Reynolds numbers thereby results in an orifice whose practical range of applicability is increased (i.e., it may be used for smaller Re_D). The primary purpose of this investigation is, therefore, to experimentally determine the values of the discharge coefficient for various conic entrance orifices and thereby assess their adequacy for flow measurement over an unusually wide range of Reynolds numbers, from the laminar region into the turbulent region.

A secondary objective is to investigate, analytically, modifications to the conic entrance orifice which might further extend the range of Re_D for which orifice flow measurement is practicable.

The conic entrance orifice has been selected by the International Standards Organization (ISO), Working Group ISO/TC30/WG10, as a recommended ISO standard when flows have pipe Reynolds numbers in the region shown in Table I. The results of this investigation, in addition to the test results of similar investigations by four leading manufacturers of flow measurement equipment, will be made available to the Fluid Meters Research Committee of the American Society of Mechanical Engineers, which will aid the U.S.A. committee for ISO/TC30 to establish its position as to the adequacy of the conic entrance orifice as an international standard for low Reynolds number flow measurements.

TABLE I - RANGE OF PIPE REYNOLDS NUMBERS AS
A FUNCTION OF DIAMETER RATIO β

β	Minimum Re_D	Maximum Re_D
0.1	40	20000
0.2	40	40000
0.3	60	50000
0.4	120	50000
0.5	260	50000

SOME THEORETICAL BACKGROUND

The theoretical equations for liquid flow through a conic orifice are normally obtained in the same fashion as for any other differential pressure meter. No allowance is made for viscous effects, a flat velocity profile is assumed, and the liquid is considered incompressible. Using this model, the fundamental equations are those of mass conservation,

$$\rho V_1 A_1 = \rho V_2 A_2$$

and energy conservation at constant elevation:

$$P_1 + \frac{1}{2}\rho V_1^2 = P_2 + \frac{1}{2}\rho V_2^2$$

Denoting the ratio of the orifice diameter, d , to the pipe diameter, D , by β , it is a matter of simple algebra to solve the above equations for the theoretical mass flow rate:

$$m_t = \rho V_2 A_2 = \pi d^2 \left(\frac{2\rho(P_1 - P_2)}{1 - \beta^4} \right)^{\frac{1}{2}}$$

If the actual mass flow rate is denoted by m_a , then the discharge coefficient is defined by:

$$C_d = \frac{m_a}{m_t}$$

Hence, if the values of d , D , and ρ are known, measurement of the difference between upstream pressure (P_1) and the pressure of the fluid issuing from the orifice (P_2) will permit determination of m_t . The actual flow rate is then predictable if C_d is known.

Although a more complete, general theory of fluid flow is manifest in the Navier-Stokes equations, these equations have never been solved exactly for flow through an orifice. The preceding, simplified method has proven most practical for measuring turbulent flows, for C_d is then nearly constant. It is in the laminar, or low Reynolds number domain that

the dependence of C_d on Re_D becomes pronounced. In this circumstance, one must know the value of Re_D in order to predict C_d and, hence, m_a . But m_a must be known in order to calculate Re_D . The lamentable situation thus arises whereby one must know m_a in order to predict m_a . With this realization, the desirability of an orifice flowmeter whose discharge coefficient exhibits only slight change with changes in Re_D in the laminar region is immediately evident.

EXPERIMENTAL PROGRAM

Test Equipment

The geometry of a conic entrance orifice plate is depicted by Figure 1. The labels on the figure identify parameters whose specifications are listed in Appendix A. Figure 2 is a photograph of the upstream face of one of the conic entrance orifice plates used in the experiments. The conic entrance is accented by the light reflected from it.

Twelve orifice plates were tested in all. Five were manufactured by Daniel Industries, Inc., and seven by Taylor Instrument Division, Sybron Corporation. Two inch piping (70" upstream, 10" downstream) was supplied by each manufacturer for use with their respective orifices. The orifice-to-pipe diameter ratio (β) had nominal values of 0.1, 0.2, 0.3, 0.4, and 0.5. The dimensions of these plates, as well as the required specifications, are listed in Appendix A. It should be noticed that the manufacturers evidently found certain specifications difficult to meet.

Two centering dowels protruded from the flanges on the Daniel piping so that the outside diameter of an orifice plate (as depicted in Figure 2), when held flush with the dowels, would be concentric with the piping. The Taylor flanges and orifices had matching pairs of holes in which centering pins (see Figure 3) were to be placed to assure concentricity. A paper

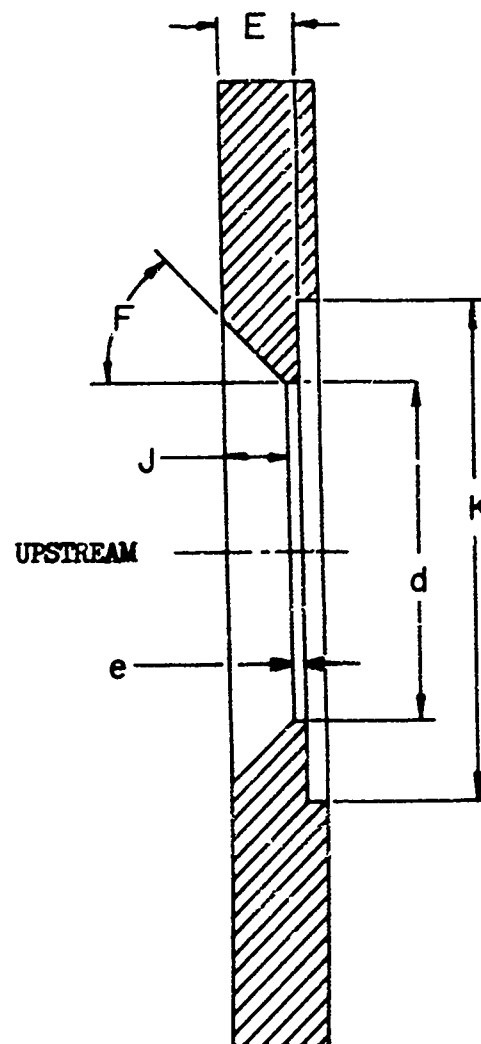


FIGURE 1 - SECTION OF CONIC ENTRANCE ORIFICE
(Specifications in Appendix A)

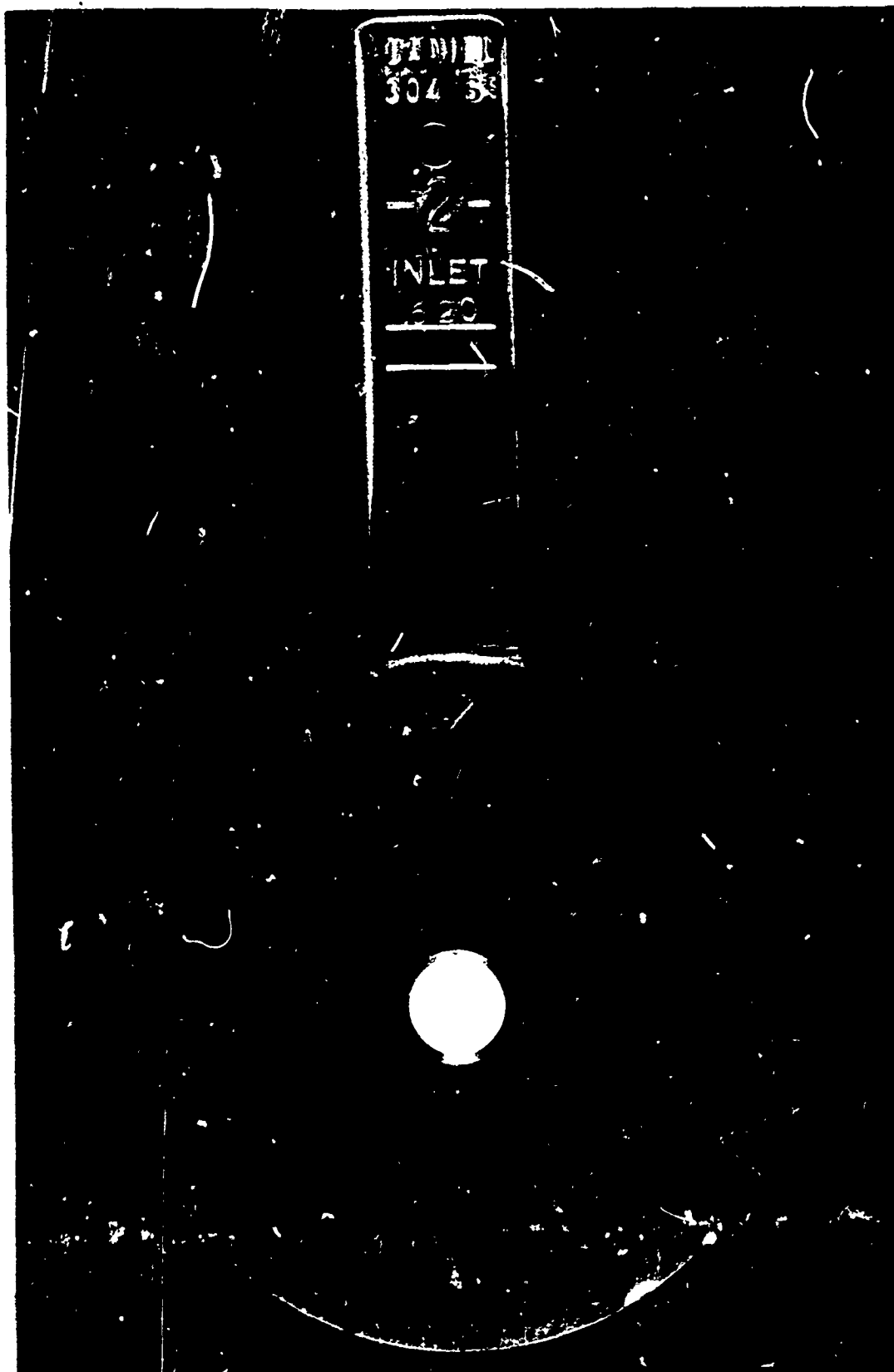


FIGURE 2 - UPSTREAM FACE OF CONIC ENTRANCE ORIFICE

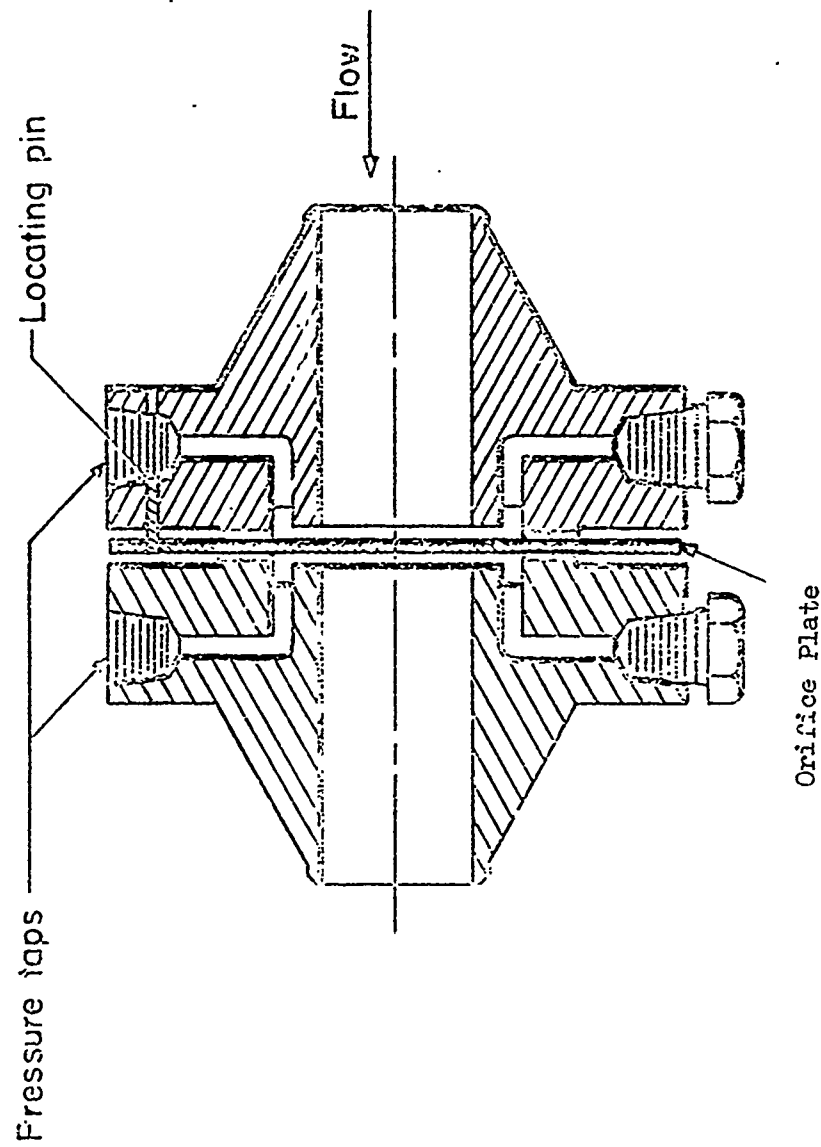


FIGURE 3 - CROSS SECTION DIAGRAM OF TAYLOR FLANGE ASSEMBLY

by Miller and Kneisel.¹ points out that eccentricity of orifice with piping may effect considerably the discharge coefficient, hence necessitating these precautions.

In order to attain the low Reynolds numbers requisite to this investigation, while maintaining differential pressure large enough to permit accurate determination of C_d , it was necessary to employ a relatively viscous fluid. On the other hand, to attain the highest Reynolds numbers called for (see Table I), while avoiding pressures too high to measure on a one-hundred inch mercury manometer, considerably lower viscosities were necessary. Preliminary calculations showed that water was unsuitable for the specified range of Re_D under the restrictions on the differential pressure range ($10'' \text{ H}_2\text{O} < \Delta P < 100'' \text{ Hg}$). Additional calculations showed that the specified ranges of Re_D (subject to the restrictions on ΔP) could be covered through the use of two oils of different viscosities: Navy Special Fuel Oil for low Re_D , and the Navy's distillate fuel for the higher values of Re_D .

Since both the water and the mercury manometers used in these tests required water filled input leads, it was necessary to have an interface between the metered liquid (oil) and water. This was accomplished by manufacturing a pair of oil-over-water reservoirs (see Figure 4), the tops of which were fed from upstream and downstream corner pressure taps respectively (see Figure 3). The cross section areas of these reservoirs were made large enough so that changes in manometer water levels would not appreciably alter the height of the interface during testing.

Test Procedure

In order to calculate the discharge coefficient accurately, it was

¹Superscripted numbers refer to references listed in the bibliography.

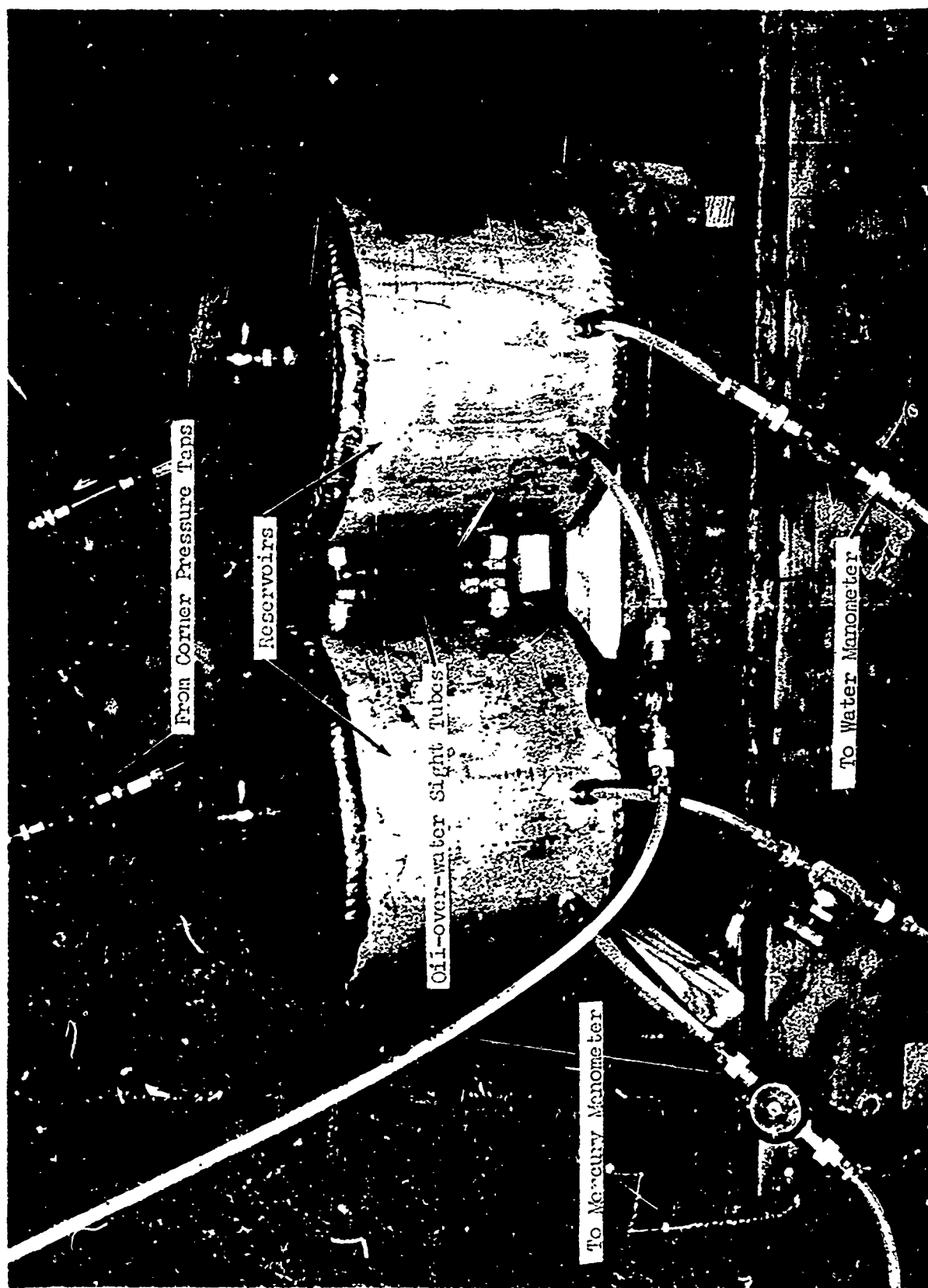


FIGURE 4 - OIL/WATER INTERFACE RESERVOIRS

NAVSECPHILADIV PROJECT A-1000

necessary to obtain precise measurements of differential pressure, fluid temperature, and mass flow rate. The latter parameter was inferred indirectly from measurements of the total weight flow, the total time of flow, and the oil specific gravity at the temperature of the test.* The differential pressure across the orifice was measured with one-hundred-inch, u-tube manometers; air over water for the low flow rates, and water over mercury for the higher flow rates. Fluid temperature was measured using iron-constantan thermocouples attached to the surface of the piping immediately preceding the orifice and about 65 inches upstream (see Figure 5). Lagging was affixed to the upstream piping (covering both thermocouple attachments) so that transient temperature conditions could be detected by the accompanying temperature disparity (i.e., at low flow rates the heated oil produced a temperature rise on the upstream thermocouple considerably in advance of the temperature rise detected near the orifice). Accurate temperature measurement was necessary to determine the oil viscosity, and hence the Reynolds number, accurately.

The accuracies sought in the measurement of primary physical parameters were chosen so that C_d might be determined within $\pm 1/4\%$. However, due to fluctuations in the flow; the necessity to measure very small differential pressures; large response times of temperature and differential pressure elements at low flow rates; and unexpected timing inaccuracies for very fast runs, a safer estimate for the mean uncertainty in the determined values of C_d is $\pm 0.4\%$ (barring systematic errors). Repeatability checks on several points substantiated this estimate. The uncertainty in Re_D was within $\pm 10\%$.

* Oil specific gravity was measured at 60°F and calculated for other temperatures using the API tables.



FIGURE 5 - TEST SET-UP

Test Results

All twelve orifice plates were tested, and the resultant data were used to calculate discharge coefficients, C_d , and pipe Reynolds numbers, Re_D . Dimensional considerations show that C_d is a function only of Re_D and the plate geometry. The results of this investigation are therefore aptly conveyed by a graph of C_d versus Re_D for each orifice plate. Such graphs are given in Figures 6 - 17.

Although the value of C_d varies with β , it is characteristic of all conic entrance orifices tested that C_d has an absolute maximum somewhere in the laminar region ($Re_D < 2000$). Although this investigation was not concerned with flow at very high Reynolds numbers, it is well known that C_d remains nearly constant for turbulent flows. It appears as though the ranges of Re_D listed in Table I are such that, at the upper limit of Re_D , C_d approaches the value it would have for fully developed turbulent flow. The lower limits on Re_D seem to have been chosen so as to exclude values of C_d that are lower than those found at the upper limit. The height of the "hump" above the turbulent value of C_d may therefore be considered as a measure of the variation in C_d over the prescribed range of Re_D . The percentage variation in C_d is then gotten by dividing this variation by the mean value of C_d in the turbulent region. This information is tabulated below (for the prescribed range of Re_D).

TABLE II - PERCENTAGE VARIATION IN C_d
OVER PRESCRIBED RANGE OF Re_D

Plate	Nominal β	% Variation
Daniel	0.1	2.2
Taylor #1	0.1	1.3
Taylor #2	0.1	1.6

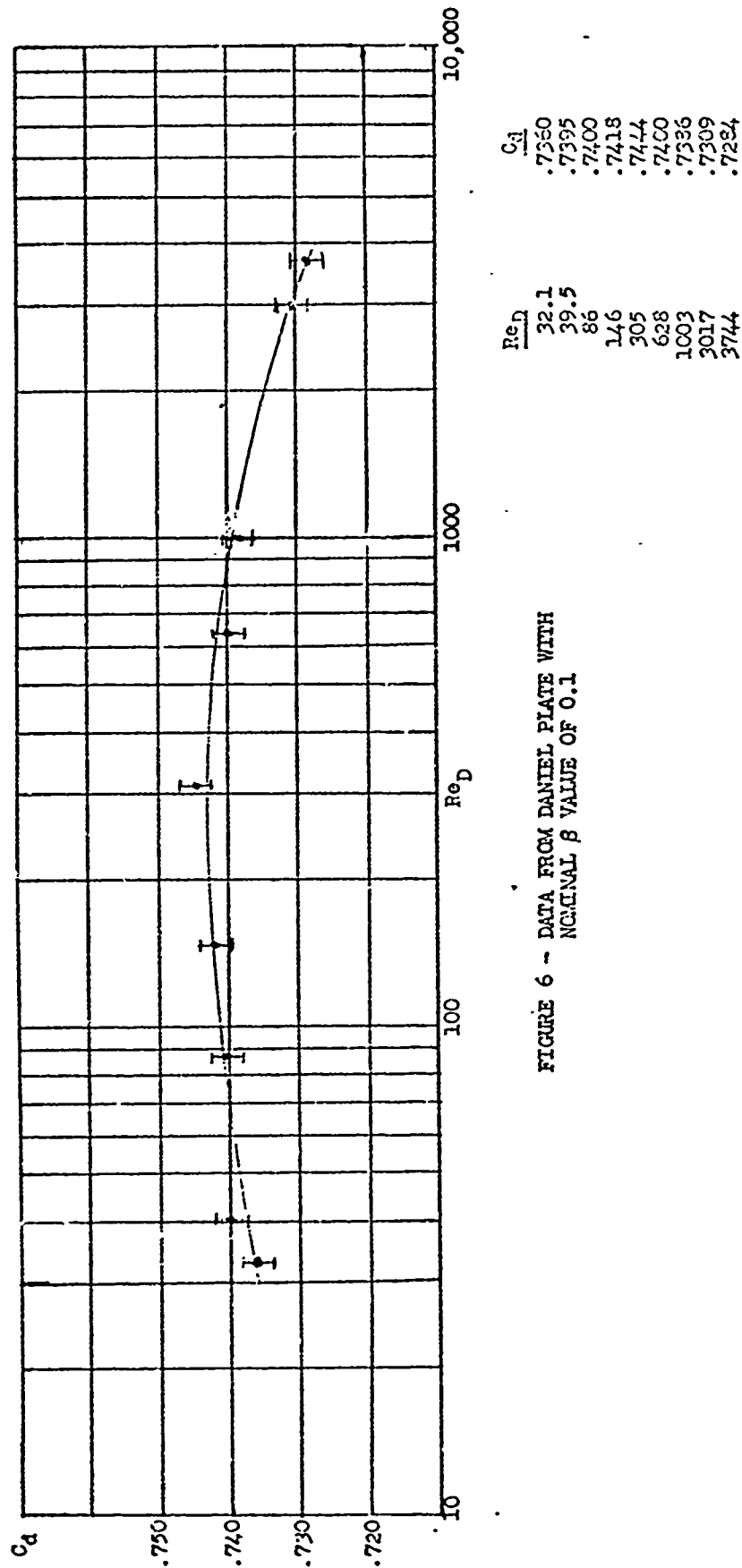


FIGURE 6 - DATA FROM DANIEL PLATE WITH
NOMINAL β VALUE OF 0.1

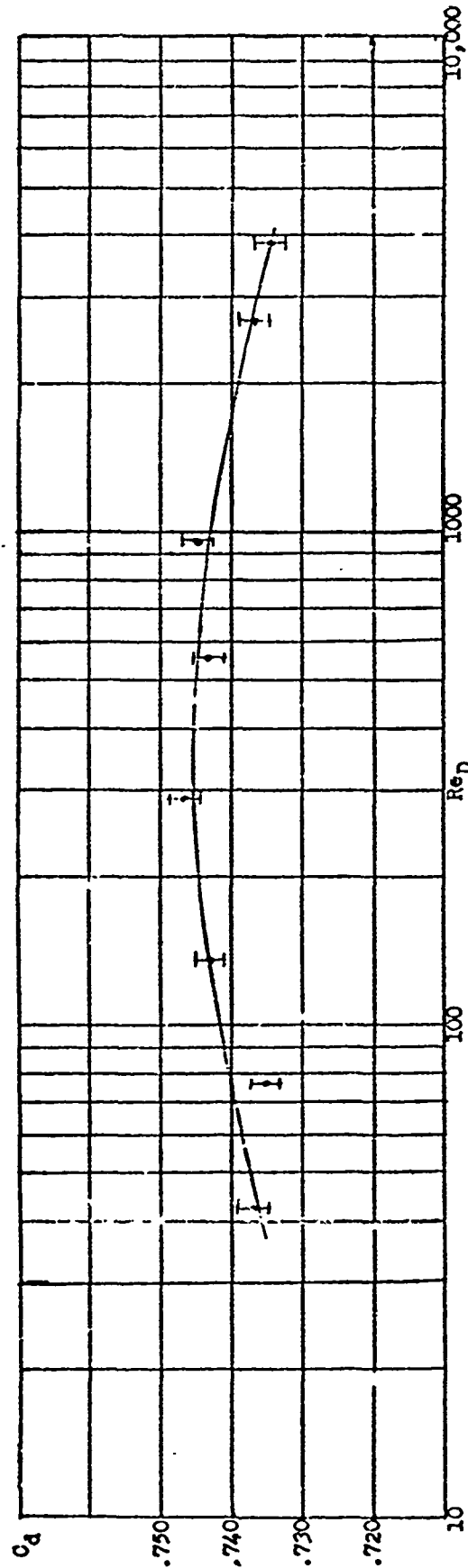


FIGURE 7 -- DATA FROM TAYLOR PLATE #2 WITH
NOMINAL β VALUE OF 0.1

Re_D	C_d
41	.7368
77	.7352
138	.7432
289	.7463
560	.7434
973	.7445
2760	.7369
3923	.7344

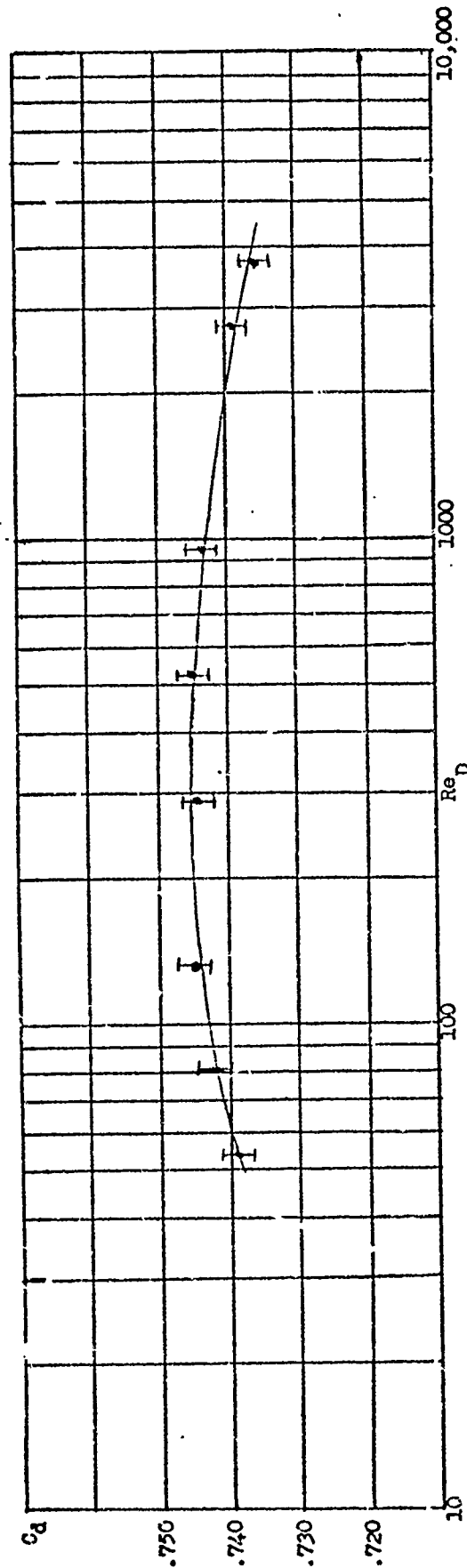


FIGURE 3 - DATA FROM TAYLOR PLATE #1 WITH
NOMINAL β VALUE OF 0.1

Re_D	C_d
54	.7392
81	.7422
133	.7448
291	.7441
531	.7452
975	.7438
2837	.7391
3875	.7359

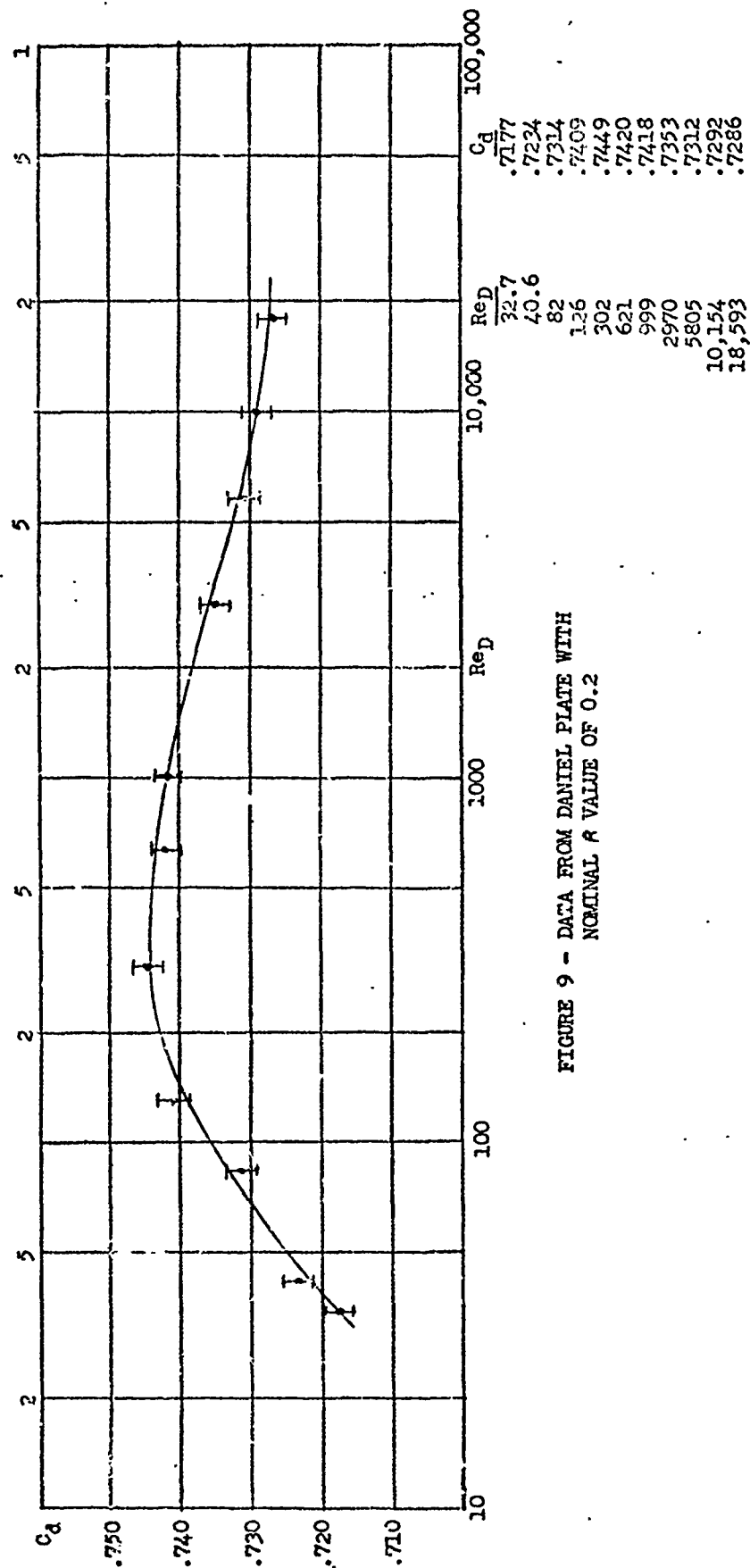


FIGURE 9 - DATA FROM DANIEL PLATE WITH
NOMINAL β VALUE OF 0.2

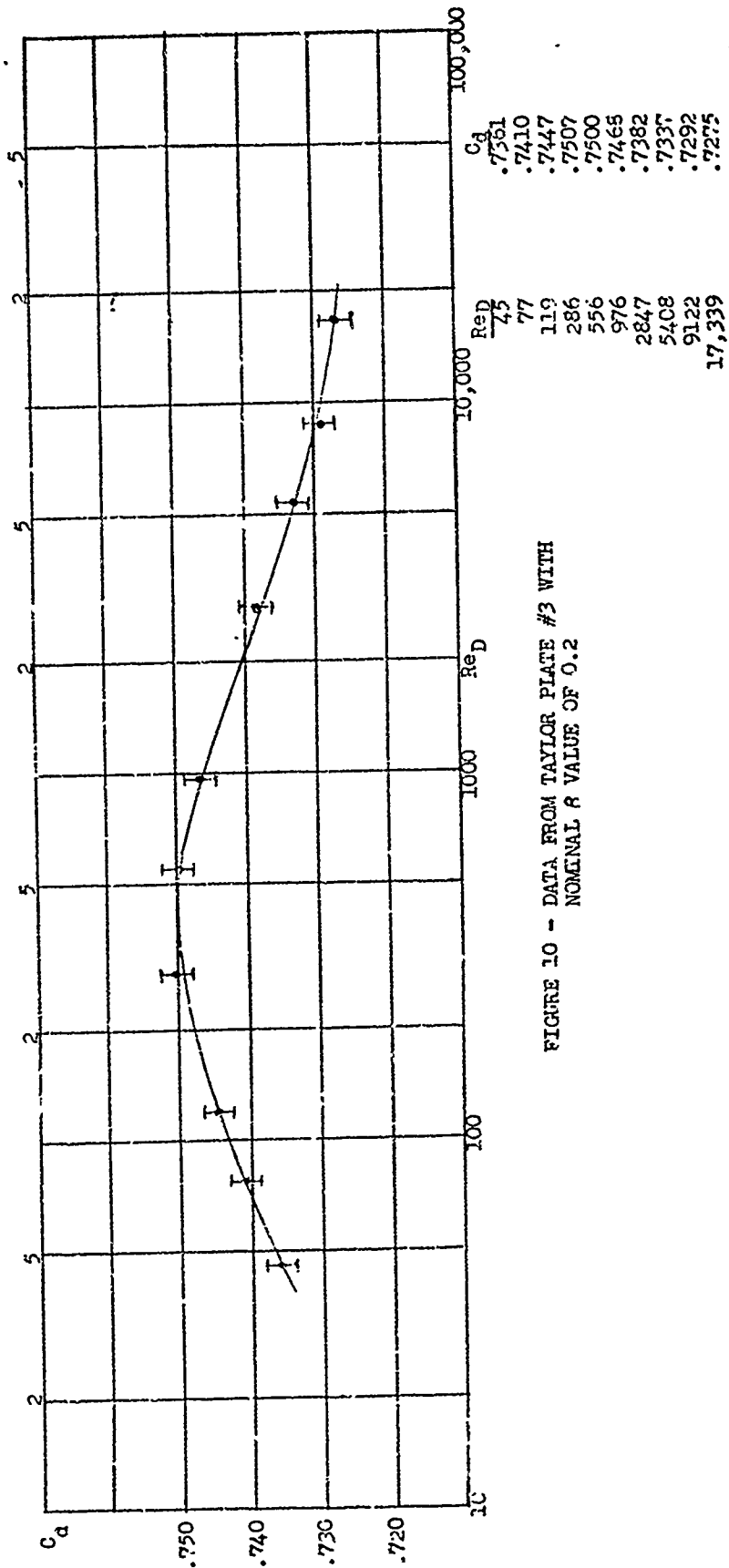


FIGURE 10 - DATA FROM TAYLOR PLATE #3 WITH
NOMINAL α VALUE OF 0.2

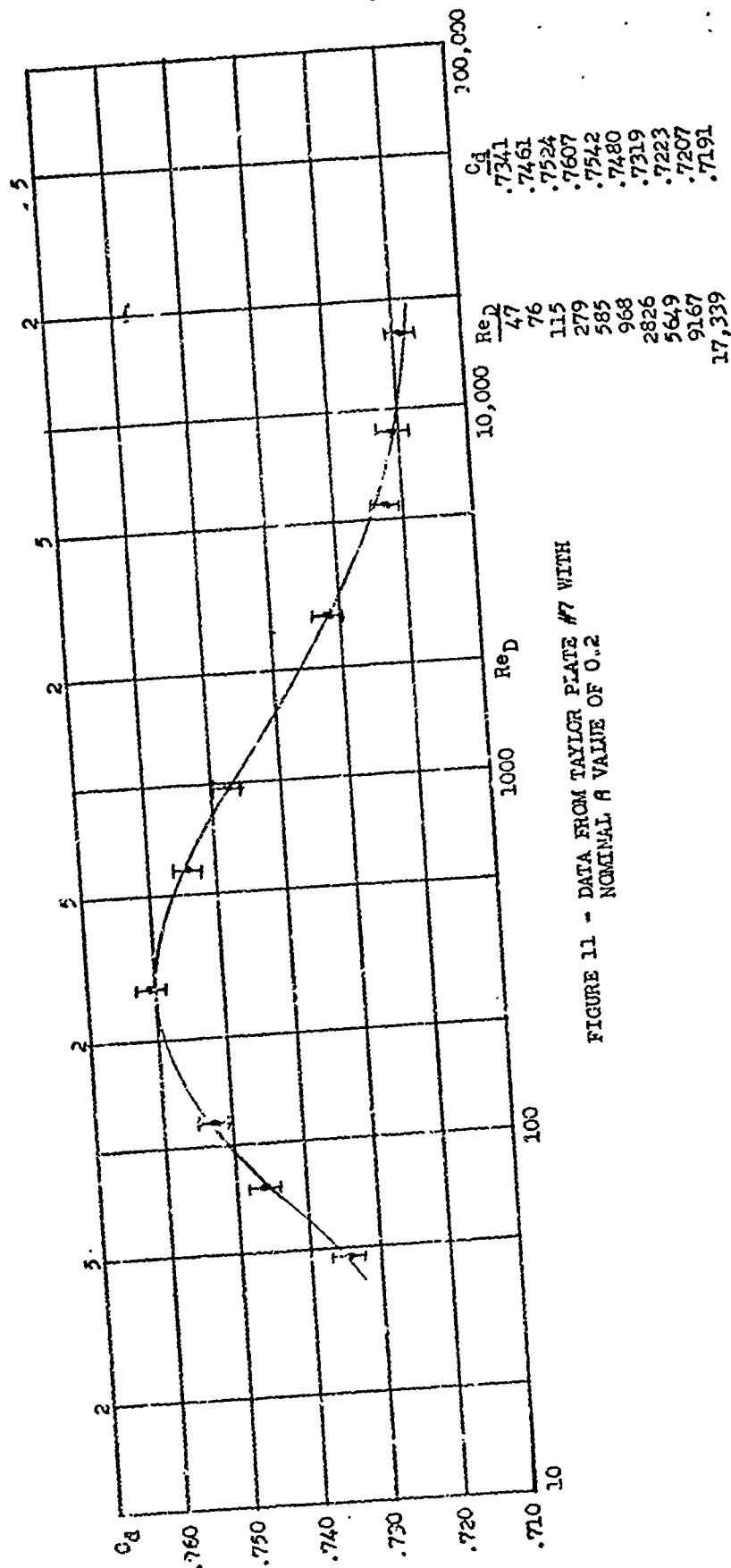


FIGURE 11 - DATA FROM TAYLOR PLATE #7 WITH
NOMINAL A VALUE OF 0.2

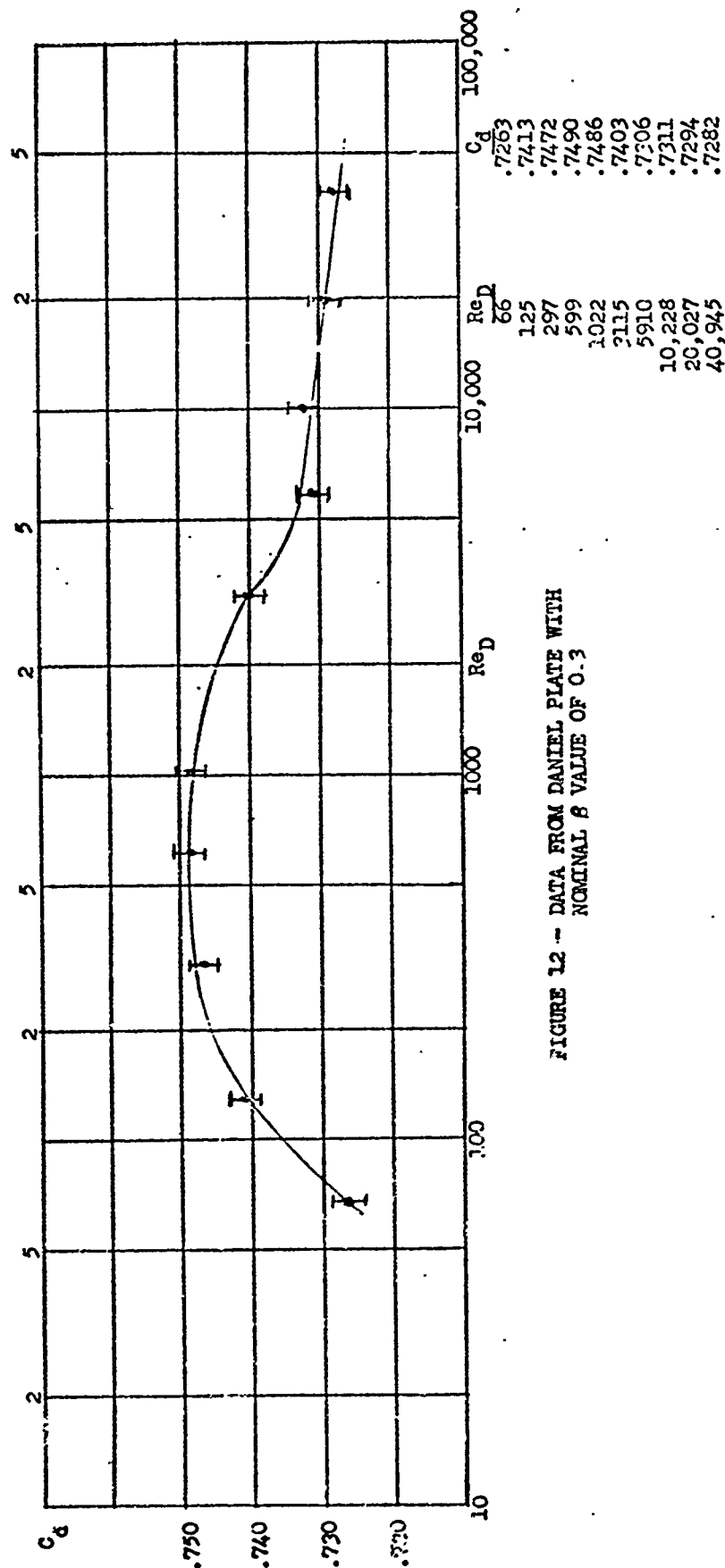


FIGURE 12 -- DATA FROM DANIEL PLATE WITH
NOMINAL β VALUE OF 0.3

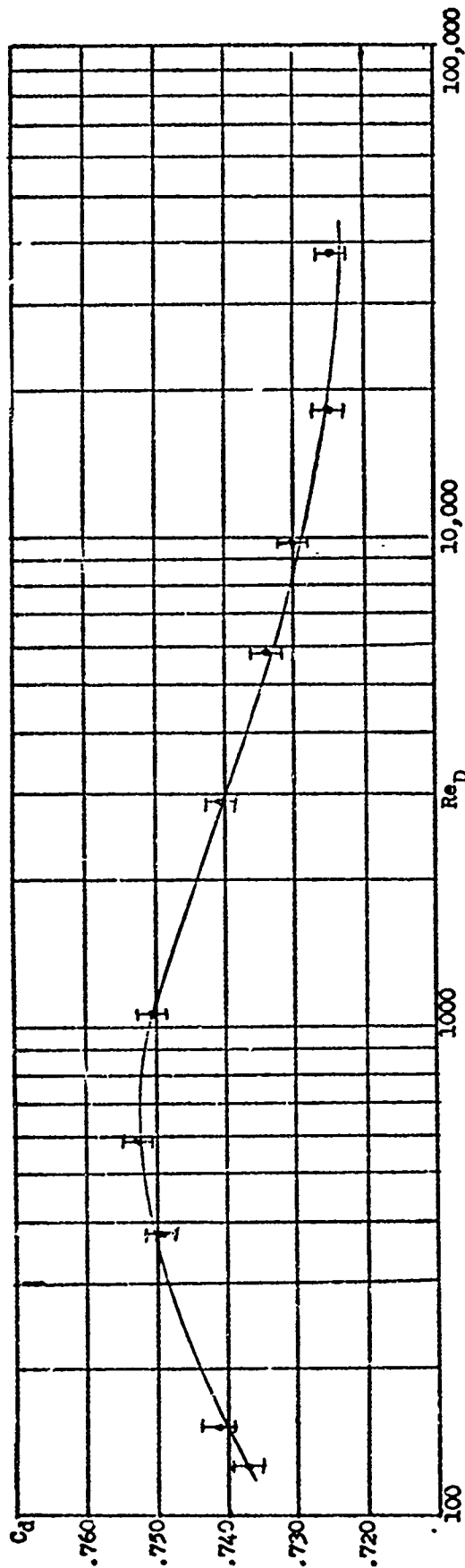


FIGURE 13 - DATA FROM TAYLOR PLATE #4 WITH
NOMINAL β VALUE OF 0.3

Re_D	C_d
123	.7366
149	.7415
369	.7496
571	.7528
1038	.7507
2870	.7405
5849	.7340
9872	.7302
18,451	.7253
38,809	.7251

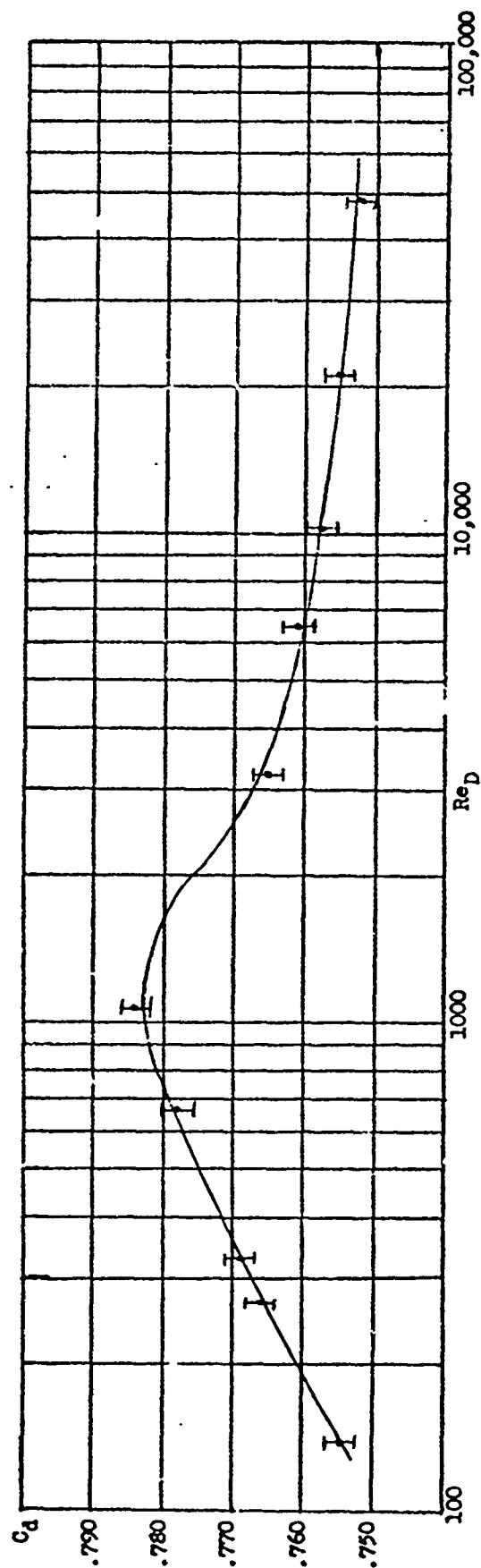


FIGURE 14 - DATA FROM DANIEL PLATE WITH
NOMINAL β VALUE OF 0.4

Re_D	C_d
136	.7549
263	.7666
324	.7692
662	.7783
1057	.7842
3179	.7654
6455	.7617
10,387	.7578
21,144	.7555
49,896	.7526

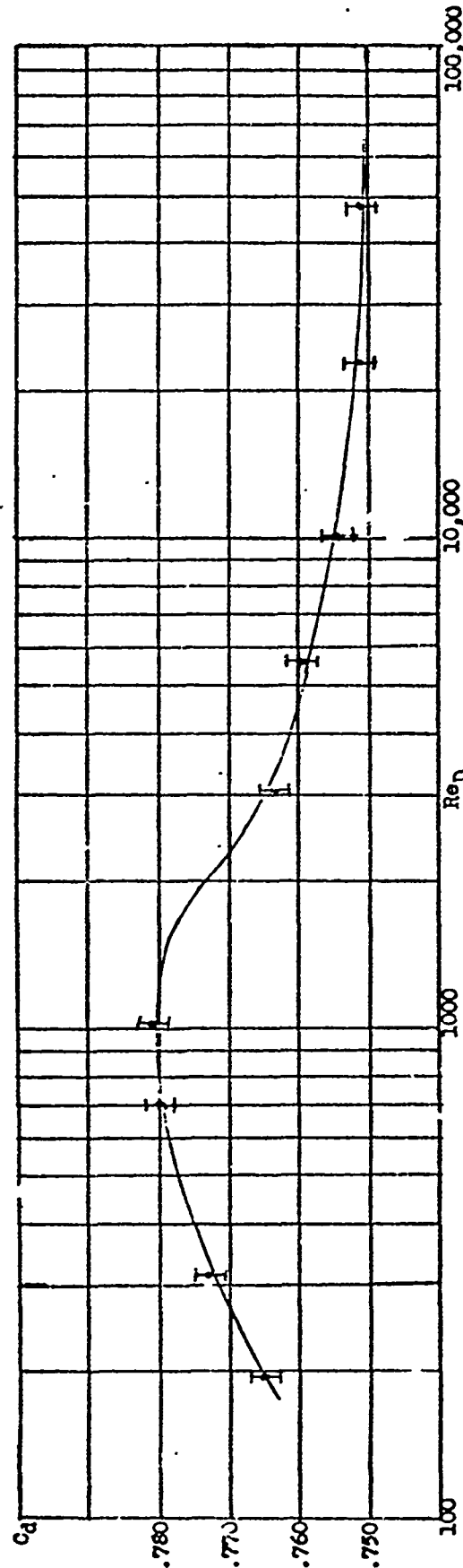


FIGURE 15 - DATA FROM TAYLOR PLATE #5 WITH
NOMINAL β VALUE OF 0.4

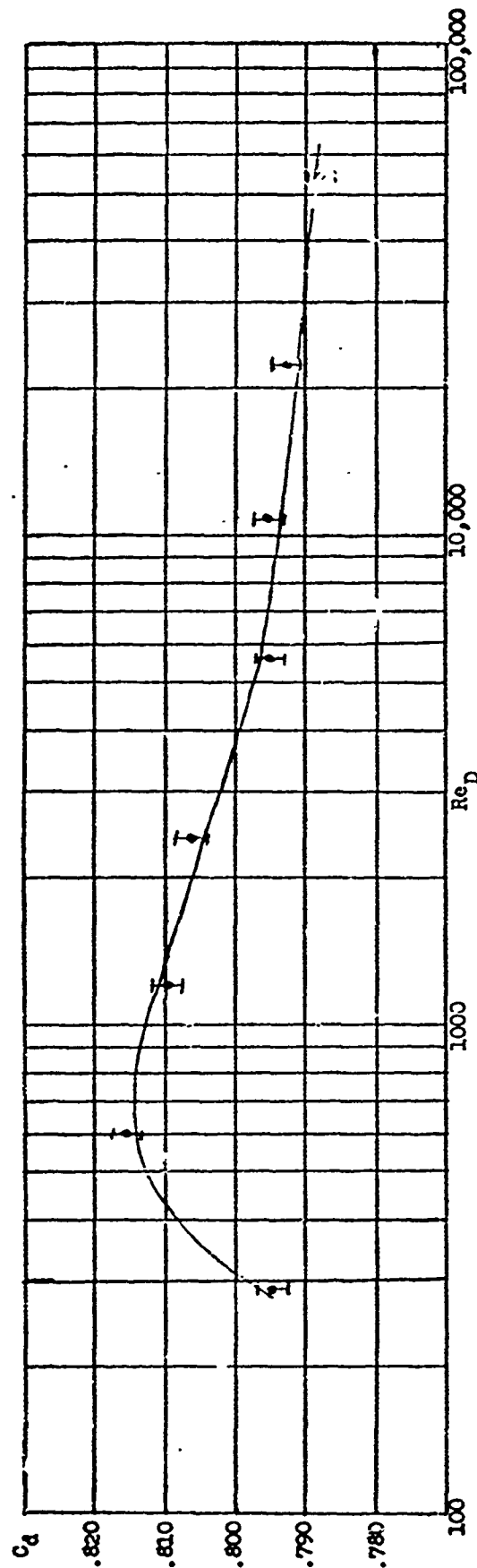


FIGURE 16 - DATA FROM DANIEL PLATE WITH
NOMINAL β VALUE OF 0.5

Re_D	C_d
291	.7953
604	.8157
1191	.8100
2401	.8067
5594	.7955
10,890	.7956
22,883	.7932
52,774	.7881

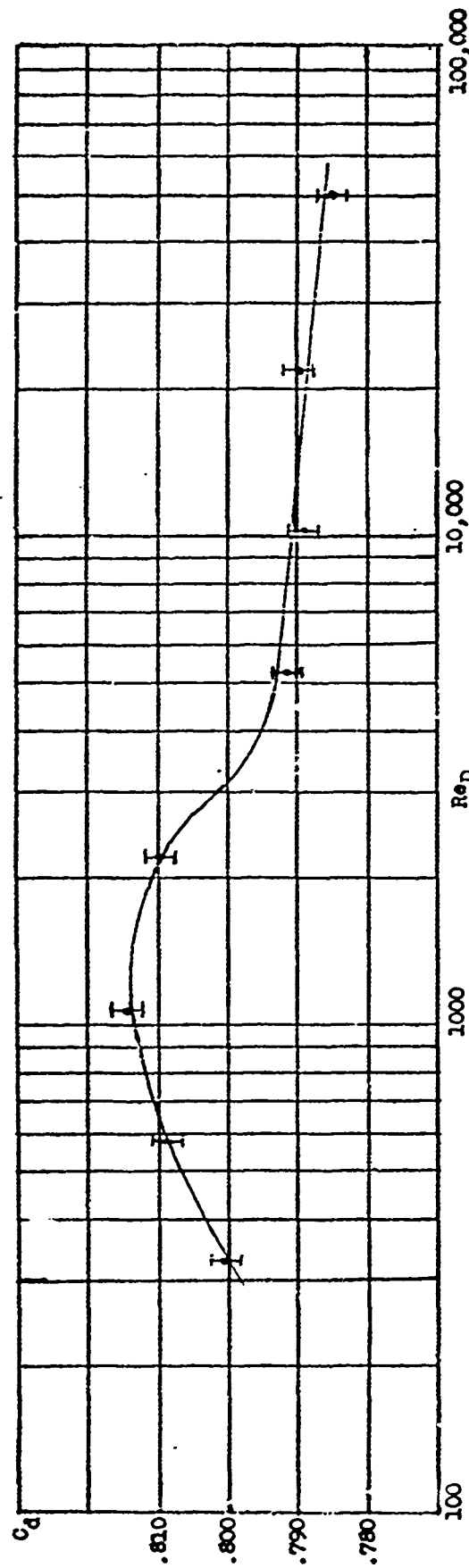


FIGURE 17 - DATA FROM TAYLOR PLATE #6 WITH
NOMINAL β VALUE OF 0.5

Re_D	C_d
321	.8002
572	.8086
1078	.8143
2197	.8099
5229	.7913
10,375	.7839
22,167	.7697
50,589	.7843

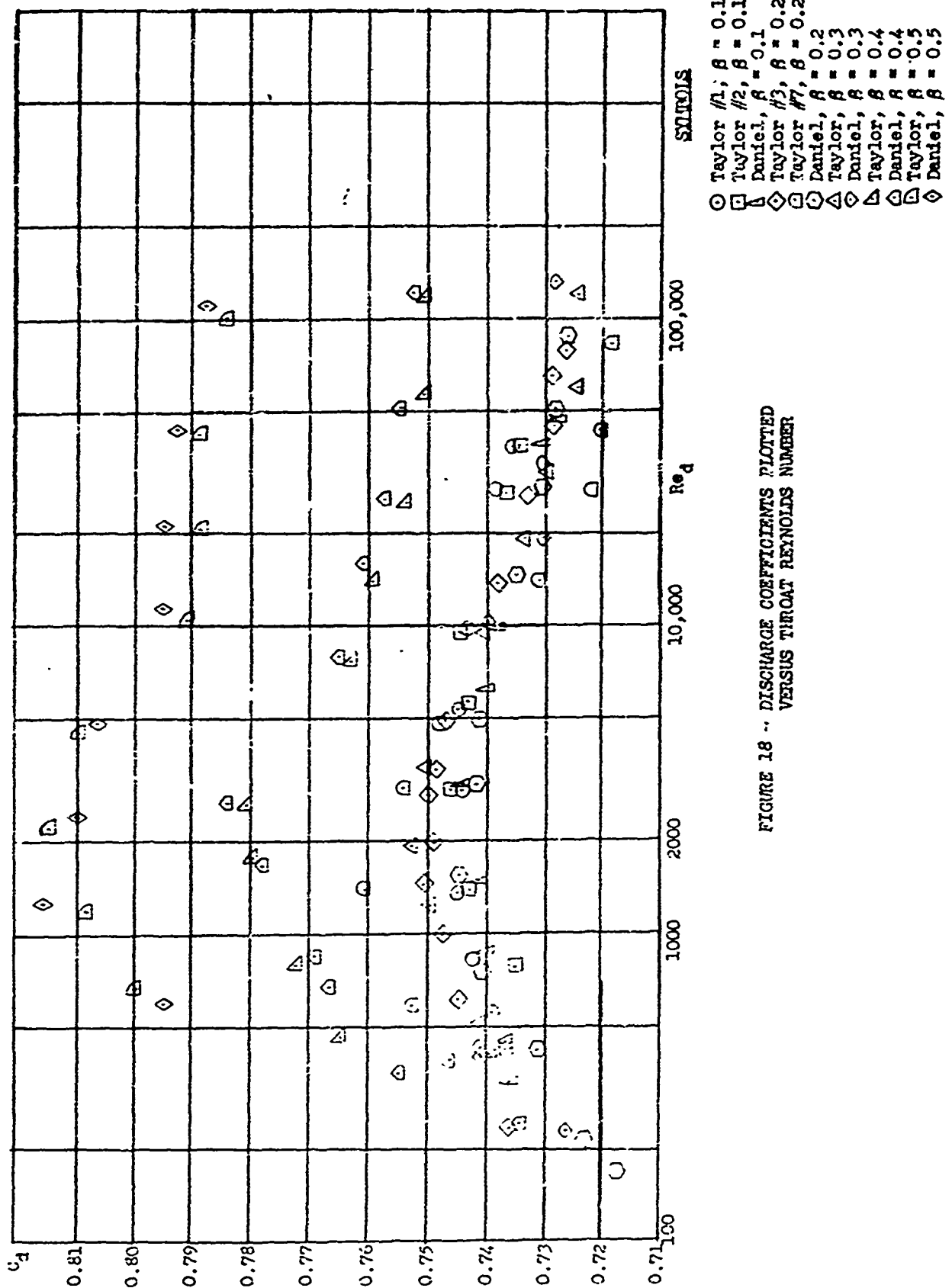
TABLE II - PERCENTAGE VARIATION IN C_d OVER
PRESCRIBED RANGE OF Re_D (Continued)

Plate	Nominal β	% Variation
Daniel	0.2	3.0
Taylor #3	0.2	3.2
Taylor #7	0.2	5.8
Daniel	0.3	3.1
Taylor	0.3	3.3
Daniel	0.4	4.2
Taylor	0.4	4.0
Daniel	0.5	3.5
Taylor	0.5	3.8

It is interesting to notice that Taylor Plate #7, whose discharge coefficient exhibits an unusually large % variation, is also characterized by a throat thickness (dimension "e" in Appendix A) which is more than four times the value called for by specifications. More generally, the plates with smaller diameter ratios appear to show less deviation in C_d . For practical purposes, when a conic orifice is used over the specified range of Re_D , C_d should be considered to have the value lying midway between the extreme values of C_d , thereby having an uncertainty of one-half of the % variation listed above (i.e., for $R = 0.1$, C_d might be considered accurate within $\pm 1\%$). It should also be noted that, for the low Reynolds number range of data compiled by the American Society of Mechanical Engineers² on square edged orifice plates, there is a greater % variation in C_d than was found for the conic entrance orifices described herein (for the same Reynolds number range).

Although all of the test results are embodied in Figures 6-17, it is nonetheless informative to plot the discharge coefficient versus the Reynolds number based on the orifice diameter, Re_d (throat Reynolds number). Figure 18 is such a plot, and the similarity of the curves for the various orifices is quite apparent. In particular, the value of Re_d for which C_d is a maximum is essentially the same for all the orifices tested, regardless of the value of β . The implication is that Re_d is a physically more meaningful dimensionless group against which to plot C_d . This follows if one interprets the change in sign of the slope of the graph as signifying the transition from laminar to turbulent flow in the orifice. With this assumption, Figure 18 indicates that Re_d , rather than Re_p , more completely characterizes the nature of the flow through the orifice, with the effect of β being merely to lower or raise the characteristic curve.

A more exact treatment of energy conservation than the usual application of Bernoulli's equation may be used to estimate the dependence of the discharge coefficient on β . Appendix C should be consulted for such an analysis.


FIGURE 18 -- DISCHARGE COEFFICIENTS PLOTTED
VERSUS THROAT REYNOLDS NUMBER

ANALYSIS

Although simplicity characterizes the morphic description of an orifice plate, its dynamic behavior is nothing less than complicated. In fact, an exact solution for the flow of a real fluid through an orifice has never been attained. To accomplish this, the Navier-Stokes equations would have to be solved for the appropriate boundary conditions (i.e., the velocity vanishes on all solid surfaces). However, the nonlinearity of these equations, as well as the discontinuous boundary conditions has made their solution unfeasible. A more general and more qualitative approach must be employed if the performance of the conic orifice is to be "understood". The most reasonable aim of such an undertaking is to decipher precisely which modifications to the plate geometry will result in a lesser variation of C_d in the low Reynolds number domain.

Dimensional analysis of the parameters which characterize incompressible flow through a conic orifice shows that a complete description of any test with a conic orifice is expressible in terms of the dimensionless numbers: C_d , Re_D , β , F , $\frac{e}{d}$ and $\frac{J}{d}$ (the last three symbols refer to Figure 1). Further, if the viscosity is neglected, then Re_D is no longer necessary. The important conclusion is that, for an ideal (inviscid) fluid, C_d is a function of the plate geometry and β alone. Since C_d would be constant for all flow rates were the fluid inviscid, it must be the viscosity which causes the characteristic "humps" in Figures 6 - 17.

It is instructive to solve the problem of ideal fluid flow (potential flow) through an ordinary, square edged orifice. This can be done for the case of vanishing β , with the added assumption of uniform mass flux through the plane of the orifice. (These assumptions greatly facilitate solution.) The problem is worked out in Appendix B. The solution thus obtained predicts a discharge coefficient of approximately 0.65. Under

the assumptions made, the direction of the fluid velocity at the orifice edge necessarily makes an angle of about 45° with the pipe axis. To assess the validity of this model, the experimental results must be consulted. The average value of the discharge coefficient for slightly turbulent flow ($Re_D \sim 2000$) through an orifice with $R = 0.1$ is about 0.61^2 . Although the prediction given above is about 7% too high, it should be noted that the analysis in Appendix B shows that the exact prediction is actually less than 0.65 (perhaps by several per cent). It is also interesting to note that 45° is the optimum edge bevel angle for conic entrance orifices with small R . Based on the above results, it is clear that the analysis and assumptions made form a reasonably accurate description of the actual flow through a square edged orifice with small diameter ratio (R) in the region of low turbulence ($Re_D \sim 2000$).

Although the above results are gratifying, they do not point directly to a means of improving the conic entrance orifice. Still, it should be kept in mind that the more closely the test conditions approach the ideal, the more nearly C_d might be expected to remain constant. Before discussing plate modifications which might be expected to result in more nearly ideal boundary conditions, the reason for the improved performance of the conic entrance orifice as compared to a square edged orifice should be elaborated.

The exact solution of the Navier-Stokes equations for the steady flow of a real, incompressible fluid (liquid) along a converging, plane-walled channel was obtained by G. Hamel in 1916³. Although the solution is

very complicated mathematically, qualitatively the results are that, for Re_D much larger than 1 (perhaps several hundred), the flow is essentially like that of an ideal fluid (i.e., potential flow). Although this solution is for the two dimensional case, it is very reasonable to assume that its essential characteristics would be found in the exact solution for converging flow in a cone. Thus, it would be expected that the introduction of a conical entrance to a square edged orifice could be considered as a perturbation to the flow whose effect is to bring the flow pattern into closer correspondence to the potential flow solution. It should be remembered that this reasoning is valid only for $Re_D \gg 1$.

Mathematically speaking, the only requirement for potential flow is that the curl of the velocity vanish throughout the region under consideration. Physically, non-zero curl is created in regions of fluid shear stresses which are attributable to non-zero viscosity plus the no-slip boundary condition (i.e., $\vec{v} = 0$ on all surfaces). Since the fluid viscosity is something that cannot be eliminated, it is only through the boundary conditions that the curl of the velocity might be minimized. For practical values of Re_D , zero curl is never a good approximation downstream from an orifice plate. Therefore, only modifications to the upstream boundary conditions will be considered here.

Examination of Figures 6 - 17 shows that increasing β has an undesirable effect on the behavior of C_d . Since the magnitude of β is indicative of the relative proximity of the pipe wall to the orifice, it is reasonable to surmise that the nearness of bounding surfaces to the orifice entrance enhances non-ideal performance. It appears that a step

U toward ideal performance would involve a decrease in the surface area near the conic entrance. Aside from the pipe walls, the only other surface near the conic entrance is the upstream face of the orifice plate itself. This may therefore be accomplished in a straightforward manner by simply recessing that portion of the face of a conic entrance orifice (Figure 1) which is nearest the orifice entrance. A conic entrance orifice plate thusly modified might be called a "protruding conic edge" orifice plate, a diagram of which is Figure 19. It should be emphasized that, to the best of the author's knowledge, such an orifice does not presently exist, and Figure 19 is merely one possible design which seems worthy of investigation. The central ideal behind this type of modification is to decrease the influence that the viscous effects associated with the plate surface have on the orifice inlet velocity profile.

It should also be mentioned that, although theoretical considerations might lead to an extended range of applicability of orifice flow measurement, they also lead to the conclusion that orifice flow measurement cannot be practicable in the limit of very small Reynolds numbers ($Re_D \lesssim 1$). Algebraic manipulation of the exact solution for slow, viscous flow through a slit⁴ shows that C_d must vanish in the limit of very slow flow ($\bar{v} \rightarrow 0$). In other words, although it is reasonable to attempt to eliminate the characteristic hump in C_d vs. Re_D , it is impossible to eliminate the monotonic decline in C_d for values of Re_D to the left of the hump.

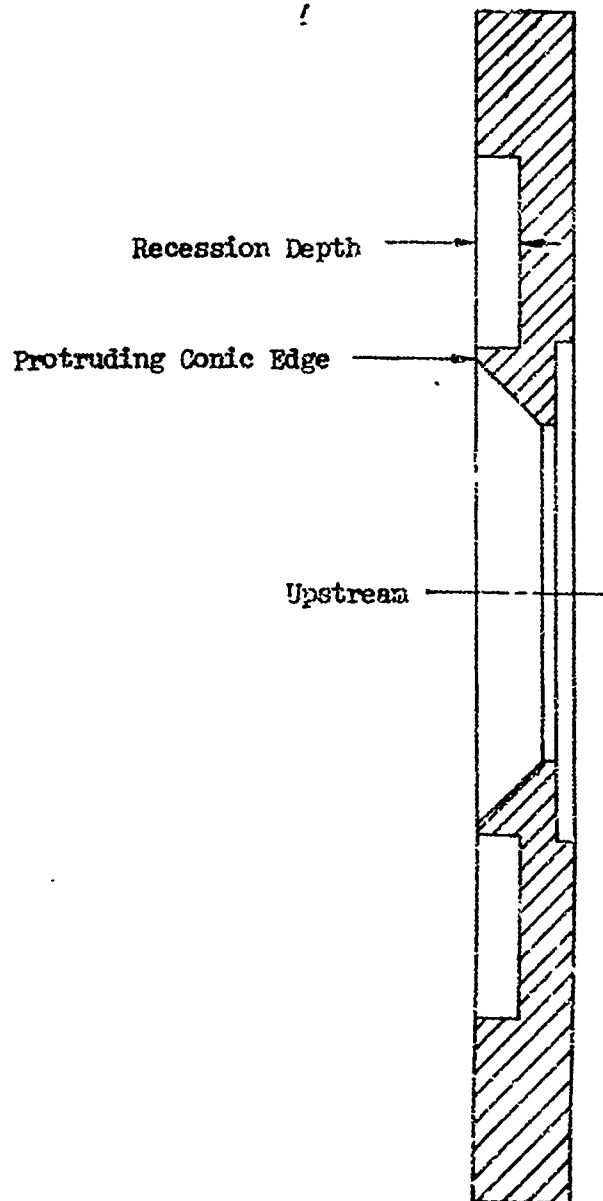


FIGURE 19 - SECTION OF PROTRUDING CONIC EDGE ORIFICE

CONCLUSIONS

While the conic entrance orifice is an improvement over the square edged orifice for flow measurement in the low Reynolds number domain (Table I), it is only for the smallest diameter ratio tested, $\beta = 0.1$, that C_d may be expected to remain constant within $\pm 1\%$. Further comparison of the data obtained in this investigation with data obtained in other investigations⁵ indicates that a plot of C_d (average) vs. β with less than 1% standard deviation (as sought by the International Standards Organization) is not feasible for the specified Reynolds number range. Also, the conic entrance orifice is not unique, since the quadrant edge orifice shows approximately the same percentage maximum variation in discharge coefficient over the specified range of Reynolds number⁶. For Reynolds numbers above 800, C_d for the quadrant edge orifice actually exhibits a lesser percentage variation.

There is reason to believe that further modification of the conic entrance orifice plate, such as the protruding edge design in Figure 18, might result in improved performance. Strict specifications would be necessary for the manufacturer of any modified plates. In particular, conformance to the specification for edge thickness (parameter "e") was found to be entirely necessary for the tested orifices (i.e., Taylor plate #7, $\beta = 0.2$, had an edge thickness of about four times the specified value, and its plot of C_d vs. Re_D was anomalous compared to the other two plates having $\beta = 0.2$). In view of the difficulties manufacturers had meeting the required specifications for the test plates, it appears as though manufacturing problems could limit practical use of the conic entrance orifice.

It should be noted that conversion from the Navy's diesel fuel oil

to Navy distillate will lower the range of Reynolds numbers encountered in certain shipboard systems. This development could give added value to the conic entrance orifice, which is well suited to low Reynolds number application.

RECOMMENDATIONS

1. The conic entrance orifice should be considered on a par with the quadrant edge orifice for shipboard flow measurement at low Reynolds numbers. Practical considerations, such as cost and manufacturers ability to meet specifications, should dictate whether the conic entrance orifice should be used instead of other (low Reynolds number) orifices.
2. Where flow rates are encountered which considerably overlap the regions listed in Table I, the conic entrance orifice is to be preferred to a square edged orifice.
3. Further investigations aimed at low Reynolds number, orifice flow measurement should study protruding conic edge designs such as that shown in Figure 19.

BIBLIOGRAPHY

1. Miller, R. W. and Kneisel, O., "Experimental Study of the Effects of Orifice Plate Eccentricity on Flow Coefficients," ASME Paper No. 68-WA/FM-1 (1968).
2. Fluid Meters - Their Theory and Application, 5th Edition, American Society of Mechanical Engineers, New York, New York, (1959).
3. Landau, L. D. and Lifshitz, E. M., Fluid Mechanics, Addison-Wesley Publishing Co., Inc., Reading, Massachusetts, (1959), p. 81.
4. Morse, P. M. and Feshbach, H., Methods of Theoretical Physics, McGraw-Hill Book Co., Inc., New York, New York, (1953), p. 1197.
5. Stöil, H. W. and Zientara, D., "The Conic Entrance Orifice Plate: An Investigation of Its Performance Characteristics," presented at Symposium on Flow: Its Measurement and Control in Science and Industry, May 9-14, 1971, Pittsburgh, Pennsylvania.
6. Bogema, M. and Monkmeyer, P. L., "The Quadrant Edge Orifice - A Fluid Meter for Low Reynolds Numbers," ASME Paper No. 59-A-140 (1959).

NAVSECPHILADIV PROJECT A-1000

DISTRIBUTION

NAVSHIPS 2052(2), 031, 03414

DDC (12)

NAVSEC 6140C, 6153, 6153E4(2), 6141, 6153E9

NAVSHIPRANDLAB ANNA

NAVSECPHILADIV 6760, 6761, 6761C(10), 6763,
6711D02, 6711F(2)

APPENDIX A

SPECIFIED AND MEASURED VALUES OF
CONIC ENTRANCE ORIFICE PLATE DIMENSIONS

DIMENSIONAL COMPARISONS (INCHES)

Nominal Beta	Dimension Designation : (See Figure 1)	Taylor Plate	Taylor Plate	Required Spec.	Daniel Plate
.10		#1*	#2		
	E	.1180	.1181	$\frac{.124}{.126}$.1278
	F	45°	$45^{\circ} 14'$	$45^{\circ} \pm 1.5^{\circ}$	$45^{\circ} 0'$
	J	.0125	.0194	$\frac{.016}{.018}$.017
	e	.0035	.0021	.004	.008
	d	.2052	.2065	$\frac{.2075}{.2065}$.2972
	K	.4144	.4097	$\frac{.4240}{.4140}$.4165
	Actual Beta	.0990	.0996		.1004
.20		#3	#7		
	E	.1183	.1204	$\frac{.124}{.126}$.1265
	F	$45^{\circ} 40'$	$45^{\circ} 0'$	$45^{\circ} \pm 1.5^{\circ}$	$45^{\circ} 0'$
	J	.0388	.0496	$\frac{.038}{.036}$.0396
	e	.0100	.0375	.009	.0104
	d	.4122	.4163	$\frac{.4140}{.4130}$.4132
	K	.8285	.8440	$\frac{.837}{.827}$.8315
	Actual Beta	.1988	.2008		.2003

* Taylor numerical plate identification.

DIMENSIONAL COMPARISONS (INCHES)

Nominal Beta	Dimension Designation (See Figure 1)	Taylor Plate	Required Spec.	Daniel Plate
.30		#4		
	E	.1186	.124 .126	.1274
	F	43° 47'	43° ± 1.5°	45°
	J	.0568	.056 .058	.0535
	e	.0152	.013	.0165
	d	.6214	.6205 .6195	.6196
	K	1.2423	1.340 1.240	1.2426
	Actual Beta	.2997		.3003
.40		#5		
	E	.1186	.124 .126	.1280
	F	39° 28'	39° ± 1.5°	41° 30'
	J	.0800	.082 .080	.0872
	e	.0205	.017	.0148
	d	.8271	.8275 .8265	.8276
	K	1.6534	1.664 1.654	1.6588
	Actual Beta	.3989		.4012

DIMENSIONAL COMPARISONS (INCHES)

Nominal Beta	Dimension Designation (See Figure 1)	Taylor Plate	Required Spec.	Deniel Plate
.50		#6		
	E	.1861	<u>.1885</u> .1865	.1886
	F	32° 0'	32° ± 1°	32° 20'
	J	.1168	<u>.113</u> .111	.121
	e	.0167	.022	.0255
	d	1.0325	<u>1.034</u> 1.032	1.0323
	K	2.0665	<u>2.076</u> 2.006	2.0673
	Actual Beta	.4980		.5004

APPENDIX B

SIMPLIFIED SOLUTION FOR POTENTIAL
FLOW THROUGH AN ORIFICE

NOMENCLATURE

A - area
 a - radius or orifice
 C_d - discharge coefficient
 F - hypergeometric function
 f - a function of k
 G - a function of ρ
 J_n - Bessel function of order n
 k - integration variable
 P - pressure
 v - fluid velocity
 z - coordinate along symmetry axis

Greek

β - ratio of orifice diameter to pipe diameter
 γ - a substitution for the power series in t
 Γ - the gamma function
 θ - angle of converge of the flow at the orifice edge
 ξ - substitution for $\left(\frac{\rho}{a}\right)$
 ρ - radial cylindrical coordinate
 ρ_m - mass density
 ϕ - the velocity potential

Subscripts

o - at the plane of the orifice
 l - at the plane of the vena contracta
 r - in the radial direction
 t - total
 z - in the axial direction

The analysis that follows treats the flow of an incompressible, inviscid fluid through a common orifice. Only the upstream velocity field is treated, since the condition of zero curl, which is necessary for potential flow, is almost never a reasonable approximation downstream of an orifice. The condition of incompressible flow (a very good assumption for liquids) is expressible mathematically as

$$\vec{\nabla} \cdot \vec{v} = 0$$

The condition of zero curl permits the expression of the velocity as the gradient of a velocity potential:

That is,
$$\vec{\nabla} \times \vec{v} = 0$$

permits the velocity to be expressed as

$$\vec{v} = \vec{\nabla} \phi$$

The equation which the potential must satisfy throughout the upstream volume is therefore Laplace's equation:

$$\nabla^2 \phi = 0$$

Because the problem has cylindrical symmetry, a general mathematical expression may be used for the potential in the semi-infinite domain^{B1}:

$$\phi(r, z) = \int_0^\infty dk f(k) e^{-kz} J_0(kr) \quad \text{Equation (B1)}$$

where the form of $f(k)$ depends on the boundary conditions. If the orifice has radius a , then an obvious boundary condition is that the component of velocity normal to the plate vanish at the plate:

$$v_z(r, 0) = \frac{\partial \phi(r, 0)}{\partial z} = 0 \text{ for } a < r < \infty$$

To completely determine the solution throughout the region, the boundary

conditions must be specified over the entire bounding surface. Since the geometry does not dictate the boundary conditions at the orifice, we assume that the efflux of fluid is uniform over this surface:

$$v_z(\rho, 0) = \frac{\partial \phi(\rho, 0)}{\partial z} = v_{z_0} \text{ for } 0 \leq \rho \leq a$$

Noticing that

$$\frac{\partial \phi}{\partial z}(\rho, 0) = \int_0^\infty dk k f(k) J_0(k\rho)$$

the boundary conditions which determine $f(k)$ are seen to be:

$$\int_0^\infty dk k f(k) J_0(k\rho) = \begin{cases} -v_{z_0} & 0 \leq \rho \leq a \\ 0 & a < \rho < \infty \end{cases}$$

To find $f(k)$ from these conditions it is necessary to employ the Hankel transform^{B2}, which states that if

$$G(\rho) = \int_0^\infty dk k f(k) J_0(k\rho)$$

then the inversion formula is:

$$f(k) = \int_0^\infty d\rho \rho G(\rho) J_0(k\rho)$$

For our problem we have

$$G(\rho) = \begin{cases} -v_{z_0} & 0 \leq \rho \leq a \\ 0 & a \leq \rho \leq \infty \end{cases}$$

so that

$$f(k) = - \int_0^a d\rho \rho (v_{z_0}) J_0(k\rho)$$

which may be evaluated using the property of Bessel functions that

$$\frac{d}{dx} [x^n J_n(x)] = x^n J_{n-1}(x)$$

which, for $n = 1$, is

$$d[xJ_1(x)] = xJ_0(x)dx$$

Letting $x = ko$, the integral for $f(k)$ becomes

$$f(k) = \frac{-v_{z0}}{k^2} \int_0^{ka} dx xJ_0(x) = \frac{-v_{z0}}{k^2} \int_0^{ka} d(xJ_1(x))$$

so

$$f(k) = \frac{-v_{z0}}{k^2} [(ka)J_1(ka) - 0] = \frac{-v_{z0} ka^2 J_1(ka)}{(ka)^2}$$

Substituting this in equation (B1) yields

$$\varphi(\rho, 0) = -v_{z0} a \int_0^\infty dk \frac{J_1(ka)J_0(k\rho)}{k}$$

This may be evaluated using relation 11.4.33 of reference B3:

$$\varphi(\rho, 0) = -(v_{z0} a) \frac{\Gamma(1/2)}{2\Gamma(1)\Gamma(3/2)} F(1/2, -1/2; 1; \left(\frac{\rho}{a}\right)^2)$$

where Γ represents the gamma function, and F is the hypergeometric function. Relation 15.1.1 of reference B3 gives the Gauss series expansion of this function for $\left(\frac{\rho}{a}\right)^2 \leq 1$.

$$\varphi(\rho, 0) = -(v_{z0} a) \frac{\Gamma(1/2)}{2\Gamma(1)\Gamma(3/2)} \cdot \frac{\Gamma(1)}{\Gamma(1/2)\Gamma(-1/2)} \sum_{n=1}^{\infty} \frac{\Gamma(\frac{1}{2} + n)\Gamma(n - \frac{1}{2})}{\Gamma(n+1)n!} \left(\frac{\rho}{a}\right)^{2n}$$

where ρ has been substituted for $\left(\frac{\rho}{a}\right)$. The problem now is essentially to expand this series, retaining enough terms for the desired accuracy, then take the negative partial derivative of the potential with respect to ρ . By definition, this will result in an approximation of the radial velocity component over the plane of the orifice. The gamma functions are tabulated and the series expansion is straightforward.

$$\phi(\rho, 0) = \frac{-v_{z0} a}{2\pi} \left[-2\pi + \frac{\pi}{2} \xi^2 + \frac{2\pi}{32} \xi^4 + \frac{45\pi}{1152} \xi^6 + \frac{1575\pi}{73728} \xi^8 + \frac{99225\pi}{7372800} \xi^{10} + \dots \right]$$

Recalling that $\frac{\partial \xi}{\partial \rho} = \frac{1}{a}$, and $\frac{\partial \xi}{\partial n} = \frac{\partial \xi}{\partial \rho} \frac{\partial \rho}{\partial n}$, we have:

$$v_r(\rho, 0) = \frac{\partial \phi(\rho, 0)}{\partial n} = \frac{-v_{z0}}{2} \left[\xi + .375\xi^3 + .2344\xi^5 + .1709\xi^7 + .1346\xi^9 \right] \text{Equation (B2)}$$

Letting γ represent the series terms in the brackets, the velocity profile on the plane of the orifice may be expressed as:

$$\vec{v}_0 = v_{z0} \left(\hat{z} - \frac{\gamma}{2} \hat{r} \right)$$

where \hat{z} and \hat{r} are unit vectors in the axial and radial directions respectively.

Since we assume potential flow, the total pressure is a constant throughout the fluid, and depends on the usual (static) pressure, P , and velocity as follows:

$$P_t = P + \frac{1}{2} \rho_m v^2$$

The statement that this is a constant is equivalent to stating that energy is conserved. The remaining conservation laws which pertain are momentum conservation and mass conservation. We apply these laws between the plane of the orifice and the plane of the vena contracta, with the added assumptions that there is no flow through the radial walls of our control volume (a cylinder) and that the pressure in the plane of the vena contracta is a constant and is in fact the pressure which is measured in a real orifice test. Assuming further that the velocity profile in the vena contracta is flat, the area of the vena

contracta may be calculated. The ratio of this area to the orifice area will then be considered as our predicted value of the discharge coefficient.

For the general expression of momentum conservation page 13 of reference B4 may be consulted. For this problem, we denote the orifice plane by 0 and the plane of the vena contracta by 1. Momentum conservation becomes:

$$\int_0^a [P_t + \frac{1}{2}\rho_m v_{z_0}^2 - \frac{1}{8}\rho_m v_{z_0}^2 \gamma^2] 2\pi r dr = \int_0^b [P_t + \frac{1}{2}\rho_m v_{z_1}^2] 2\pi r dr + \int_b^a P_1 2\pi r dr$$

where the radius of the vena contracta is b. Letting A denote area we get

$$- \frac{A_0 \rho_m v_{z_0}^2}{4} \int_0^1 \gamma^2 \xi d\xi = - (P_t + \frac{1}{2}\rho_m v_{z_0}^2) A_0 + (P_t + \frac{1}{2}\rho_m v_{z_1}^2) A_1 + P_1 (A_0 - A_1)$$

Before going further, the integral must be evaluated. Recalling the definition of γ ($\gamma = \xi + .375\xi^3 + .2344\xi^5 + .1709\xi^7 + .1346\xi^9$), the integration is cumbersome, but straightforward. The result is:

$$\int_0^1 \gamma^2 \xi d\xi = 0.5552$$

Substituting, the principle equation becomes

$$- \frac{(0.5552)}{4} \rho_m v_{z_0}^2 A_0 = - (P_t + \frac{1}{2}\rho_m v_{z_0}^2) A_0 + (P_t + \frac{1}{2}\rho_m v_{z_1}^2) A_1 + P_1 (A_0 - A_1)$$

Substituting $P_1 = P_t - \frac{1}{2}\rho_m v_{z_1}^2$ and cancelling terms gives:

$$- 0.1388 v_{z_0}^2 A_0 = - 0.5 v_{z_0}^2 A_0 + 0.5 v_{z_1}^2 A_1 + 0.5 v_{z_1}^2 (A_1 - A_0)$$

or

$$0.2776 \left(\frac{v_{z_0}}{v_{z_1}} \right)^2 = \left(\frac{v_{z_0}}{v_{z_1}} \right)^2 - \left(\frac{A_1}{A_0} \right) + 1 - \left(\frac{A_1}{A_0} \right)$$

recalling that continuity requires $v_{z0} A_0 = v_{z1} A_1$, or $\left(\frac{v_{z0}}{v_{z1}}\right) = \left(\frac{A_1}{A_0}\right)$, we obtain, on rearranging terms:

$$\left(\frac{A_1}{A_0}\right)^2 - 2.7685 \left(\frac{A_1}{A_0}\right) + 1.3843 = 0$$

Since the ratio (A_1/A_0) is just the theoretical correction to the mass flow rate predicted using Bernoulli's equation, the root of this equation is the theoretical discharge coefficient:

$$C_d \approx \frac{2.7685 \pm \sqrt{(2.7685)^2 - 4(1.3843)}}{2}$$

or

$$C_d \approx .65$$

This result should be compared to the average experimental value of C_d with $R = 0.1$, which is approximately 0.61. It should be noted that retention of higher order terms in the previously obtained (hypergeometric) series would result in a smaller predicted value for C_d . Because of the poor convergence of this series near $\alpha = a$, the exact solution (retaining all terms) is probably a few percent lower than the approximation given here. It is therefore quite clear that the analysis given above is a reasonably accurate description of the actual flow through a square edged orifice with small diameter ratio (R) in the region of low turbulence ($Re_d \sim 2000$).

The angle of convergence of the fluid velocity at the edge of the orifice may be estimated by substituting $\epsilon = 1$ into equation (B2):

$$v_r \approx v_0$$

so that the angle of convergence is approximately

$$\theta \simeq \tan^{-1} \left(\frac{v_r}{v_o} \right) = 45^\circ$$

which happens to be the optimum bevel angle for the conic entrance orifice (with $\beta = 0.1$).¹

References:

- B1 - Jackson, J. D., Classical Electrodynamics, John Wiley and Sons, Inc., New York, New York, (1962), p. 77.
- B2 - Morse, P. M. and Feshbach, H., Method of Theoretical Physics, McGraw-Hill Book Company, Inc., New York, New York, (1953), p. 962.
- B3 - Abramowitz, M. and Stegun, I. A., Handbook of Mathematical Functions, National Bureau of Standards Applied Mathematics Series 55, (1964), p. 487
- B4 - Landau, L. D. and Lifshitz, E. M., Fluid Mechanics, Addison-Wesley Publishing Company, Inc., Reading, Massachusetts, (1959), p. 13.

NAVSECPHILADIV PROJECT A-1000

APPENDIX C

CORRECTION TO DISCHARGE COEFFICIENT
DUE TO LAMINAR UPSTREAM VELOCITY PROFILE

In the analysis that follows it will be shown that the principles of energy and mass conservation can be used to derive a more exact expression for the flow rate through an orifice than that normally obtained using the Bernoulli equation for one-dimensional flow. Viscous energy dissipation will be neglected.

If ϵ denotes the internal energy per unit mass, then the energy per unit volume of the fluid is:

$$\frac{1}{2}\rho v^2 + \rho\epsilon$$

The time rate of change of this energy density is simply

$$\frac{\partial}{\partial t} (\frac{1}{2}\rho v^2 + \rho\epsilon)$$

Using the equation of mass continuity,

$$\frac{\partial \rho}{\partial t} + \vec{v} \cdot \nabla \rho = 0$$

along with Euler's equation for inviscid flow,

$$\frac{\partial \vec{v}}{\partial t} = -(\vec{v} \cdot \nabla) \vec{v} - \frac{1}{\rho} \nabla p$$

we find that

$$\begin{aligned} \frac{\partial}{\partial t} (\frac{1}{2}\rho v^2) &= \frac{1}{2}v^2 \frac{\partial \rho}{\partial t} + \rho \vec{v} \cdot \frac{\partial \vec{v}}{\partial t} \\ &= -\frac{1}{2}v^2 \vec{v} \cdot \nabla \rho - \vec{v} \cdot \nabla p - \rho \vec{v} \cdot (\vec{v} \cdot \nabla) \vec{v} \\ &= -\frac{1}{2}v^2 \vec{v} \cdot \nabla \rho - \vec{v} \cdot \nabla p - \frac{1}{2}\rho \vec{v} \cdot \nabla v^2 \end{aligned}$$

The thermodynamic definition of the differential change in enthalpy (w) is:

$$dw = Tds + \left(\frac{1}{\rho}\right)dp$$

where s is the specific entropy. We may therefore write

$$\vec{\nabla} P = \rho \vec{\nabla} w - \rho T \vec{\nabla} s$$

which, upon substitution in the expression for the time rate of change of kinetic energy, yields

$$\frac{\partial}{\partial t} \left(\frac{1}{2} \rho v^2 \right) = -\frac{1}{2} v^2 \vec{\nabla} \cdot \rho \vec{v} - \rho \vec{v} \cdot \vec{\nabla} \left(\frac{1}{2} v^2 + w \right) + \rho T \vec{v} \cdot \vec{\nabla} s \quad \text{Equation (C1)}$$

We now consider the term $\frac{\partial}{\partial t}(\rho \epsilon)$ by writing the thermodynamic relation

$$\begin{aligned} d\epsilon &= T ds - P d\left(\frac{1}{\rho}\right) \\ &= T ds + \left(\frac{P}{\rho^2}\right) d\rho \end{aligned}$$

and recalling that $w = \epsilon + \frac{P}{\rho}$, so that

$$\begin{aligned} d(\rho \epsilon) &= \epsilon d\rho + \rho d\epsilon \\ &= \left(w - \frac{P}{\rho}\right) d\rho + \rho(T ds + \frac{P}{\rho^2} d\rho) \\ &= w d\rho + \rho T ds \end{aligned}$$

which means

$$\frac{\partial(\rho \epsilon)}{\partial t} = w \frac{\partial \rho}{\partial t} + \rho T \frac{\partial s}{\partial t}$$

In the absence of heat conduction and viscous energy dissipation, the entropy per unit mass of a fluid "particle" will remain constant in time:

$$\frac{ds}{dt} = \frac{\partial s}{\partial t} + \vec{v} \cdot \vec{\nabla} s = 0$$

or

$$\frac{\partial s}{\partial t} = -\vec{v} \cdot \vec{\nabla} s$$

Likewise, the continuity equation for mass may be written:

$$\frac{\partial \rho}{\partial t} = -\vec{\nabla} \cdot \rho \vec{v}$$

the expression for $\frac{\partial(\rho \epsilon)}{\partial t}$ becomes, with the above substitutions,

$$\frac{\partial(\rho\epsilon)}{\partial t} = -\vec{w} \cdot \vec{\rho} - \rho \vec{f} \cdot \vec{v} \quad \text{Equation (C2)}$$

The time rate of change for the total energy per unit volume may therefore be written (using equations (C1) and (C2))

$$\frac{\partial(\frac{1}{2}\rho v^2 + \rho\epsilon)}{\partial t} = -(\frac{1}{2}v^2 + w)\vec{\rho} \cdot \vec{v} - \rho \vec{v} \cdot \vec{v}(\frac{1}{2}v^2 + w)$$

or, finally, using the relation $\vec{v} \cdot \vec{f} = f\vec{v} \cdot \vec{g} + \vec{g} \cdot \vec{v}f$,

$$\frac{\partial(\frac{1}{2}\rho v^2 + \rho\epsilon)}{\partial t} = -\vec{v} \cdot [\rho \vec{v}(\frac{1}{2}v^2 + w)]$$

This equation may be applied to steady state orifice flow ($\frac{\partial}{\partial t} = 0$) by integrating over some volume and transforming this volume integral to a surface integral using Gauss' divergence theorem:

$$0 = \int_{\text{volume}} \vec{v} \cdot [\rho \vec{v}(\frac{1}{2}v^2 + w)] dV = \int_{\substack{\text{enclosing} \\ \text{surface}}} \rho \vec{v}(\frac{1}{2}v^2 + w) \cdot d\vec{A}$$

Let A_1 be a plane surface normal to the pipe axis, and sufficiently far upstream of the orifice that \vec{v} is parallel to the pipe axis, and let A_2 be the surface in the plane of the orifice. Using the fact that $v = 0$ on the pipe surface and orifice surface, the above equation becomes

$$\int_{\text{pipe cross-section orifice}} (\frac{1}{2}\rho v^2 + \rho w) dA_1 = \int \rho \vec{v}(\frac{1}{2}v^2 + w) \cdot d\vec{A}_2$$

Since the aim of this analysis is to correct for the upstream velocity profile, the same simplifying (but inaccurate) assumption will be made about the flow at the orifice as is normally made in the application of Bernoulli's equation: \vec{v} is parallel to the pipe axis at the orifice.

(Actually, this assumption is more correctly applied to the vena contracta.) All that remains is to assume velocity profiles at A_1 and A_2 , and the above equations may be integrated. To keep the calculations relatively simple yet accurate, consider flow for which $Re_d > 2000$, yet $Re_D < 2000$. In this region laminar flow will be encountered at A_1 , while turbulence will exist at A_2 . The velocity profile for laminar pipe flow is well known to be a paraboloid, while a flat velocity profile has been found to be a reasonable approximation for turbulent flow. In other words

$$\text{at } A_1: v = 2\bar{v}_1 \left(1 - \frac{r^2}{R^2}\right)$$

$$\text{at } A_2: v = \bar{v}_2$$

where \bar{v} means average velocity, and use has been made of the fact that the velocity along the pipe axis is twice the average velocity for laminar pipe flow. The central equation now becomes:

$$\int_0^R 4\rho\bar{v}_1 \left(1 - \left(\frac{r^2}{R^2}\right)\right)^3 2\pi r dr + \rho\bar{v}_1 w_1 A_1 = \rho\bar{v}_2 A_2 \left(\frac{1}{2}\bar{v}_2^2 + w_2\right)$$

which upon integration gives

$$\rho\bar{v}_1 A_1 (\bar{v}_1^2 + w_1) = \rho\bar{v}_2 A_2 \left(\frac{1}{2}\bar{v}_2^2 + w_2\right)$$

mass continuity requires $\rho\bar{v}_1 A_1 = \rho\bar{v}_2 A_2$, hence

$$\bar{v}_1^2 + w_1 = \frac{1}{2}\bar{v}_2^2 + w_2$$

the enthalpy is $w = \frac{P}{\rho} + \epsilon$, so that

$$\frac{1}{2} \bar{v}_1^2 + \frac{P_1}{\rho} + \epsilon_1 = \frac{1}{2} \bar{v}_2^2 + \frac{P_2}{\rho} + \epsilon_2$$

The change in the internal energy is

$$d\epsilon = Tds - \frac{P}{\rho_2} d\rho$$

However, the fluid is being considered incompressible and isentropic, so that

$$ds = d\rho = d\epsilon = 0$$

which means that $\epsilon_1 = \epsilon_2$. The equation of energy conservation becomes:

$$\rho \bar{v}_1^2 + P_1 = \frac{1}{2} \rho \bar{v}_2^2 + P_2$$

Apply the continuity equation, $\rho v_1 A_1 = \rho v_2 A_2$,

$$\bar{v}_1 = \bar{v}_2 \frac{A_2}{A_1} = v_2 \left(\frac{d_2}{D_1} \right)^2 = \alpha^2 \bar{v}_2$$

and substituting this for \bar{v}_1 ,

$$\rho \bar{v}_2^2 \alpha^4 + P_1 = \frac{1}{2} \rho \bar{v}_2^2 + P_2$$

solving for \bar{v}_2 ,

$$\bar{v}_2 = \sqrt{\frac{2(P_1 - P_2)}{\rho(1 - 2\alpha^4)}}$$

The theoretical mass flow rate is therefore

$$m_t^i = \rho \bar{v}_2 A_2 = \pi d^2 \sqrt{\frac{2\rho(P_1 - P_2)}{(1 - 2\alpha^4)}}$$

Recalling the theoretical expression obtained on page 3 of the text, and defining a new discharge coefficient, C_d^i , we have

$$m_2 = C_d m_t = C_d' m_t'$$

$$\frac{C_d'}{C_d} = \frac{m_t}{m_t'} = \sqrt{\frac{1 - 2\beta^4}{1 - \beta^4}}$$

This correction factor is tabulated below:

β	C_d'/C_d
0.1	0.9999
0.2	0.9992
0.3	0.9959
0.4	0.9868
0.5	0.9661

The validity of the preceding analysis is brought to light by a table comparing the newly defined discharge coefficient to the usual discharge coefficient in the region which this analysis treats, $Re_d \approx 2000$. (This is where the maximum of C_d occurs, and, it is hypothesized, where the transition to turbulent orifice flow begins.)

β	$C_{d(max)}$	$C_{d'(max)}$	Measured bevel angle, F
0.1	.745	.745	$45^{\circ}05'$
0.2	.752	.751	$45^{\circ}08'$
0.3	.751	.748	$44^{\circ}24'$
0.4	.782	.772	$40^{\circ}29'$
0.5	.815	.787	$32^{\circ}10'$

These are nominal β values, and average values of $C_{d(max)}$ and F for the plates tested. For the first three plates, the bevel angle is approximately the same, and C_d' is the same (within better than 1%). For the last two β values the decreasing angle of convergence apparently results in a larger value for C_d' .

In summary, it appears as though the increased height of the hump in C_d for larger β values is due to the fact that the usual Bernoulli

equation approach does not take account of the true upstream velocity profile. It is expected that if F were the same for all values of β , the curves of C_d versus Re_d would be nearly coincident for every plate, provided the correct velocity profile were used.